J. Fluid Mech. (1990), *vol.* 214, *pp.* 185–210
Printed in Great Britain

A stability analysis for interfacial waves using a Zakharov equation

By A. DIXON†
University of New South Wales, Kensington, Australia

(Received 29 June 1988 and in revised form 8 September 1989)

An amplitude equation for weak interactions of waves is derived to describe the time evolution of disturbances on an interface between fluids of differing densities, with rigid upper and lower boundaries. This equation is analogous to the Zakharov equation for water waves and is used to investigate the stability of a periodic wave. It is found that, for small wave steepnesses, the instabilities are due to resonant quartets with perturbation wavenumbers of the order of, or less than, that of the main wave. A second instability is found for large perturbation wavenumbers and moderately high wave steepnesses. This is restricted to the case when the Boussinesq parameter is small. It is shown that this is a Kelvin–Helmholtz instability caused by a wave-induced jump in the fluid velocity across the interface.

1. Introduction

It has long been known that waves can exist on a fluid surface or interface. Water waves are the best known but large-amplitude internal waves are commonly observed on the oceanic pycnocline, or on an atmospheric inversion layer, and are often approximated by an interface separating fluids of constant, but different densities.

Periodic interfacial waves have been modelled for finite amplitudes by Holyer (1979), Saffman & Yuen (1982), Pullin & Grimsham (1983*a*, *b*), amongst others. At small wave steepnesses, assuming that the effects of the Kelvin–Helmholtz instability discussed later are negligible at these steepnesses, the stability of such a wave on a surface or interface is dictated by the existence of resonant interactions. That is, a perturbation of the form of a pair of plane waves can interact with the main wave in such a way that energy exchange can take place. These resonances occur for infinitesimal wave steepnesses when the condition

$$\omega(\boldsymbol{k}_1)+\omega(\boldsymbol{k}_2) = N\omega(\boldsymbol{k}_0) \quad \text{with} \quad \boldsymbol{k}_1+\boldsymbol{k}_2 = N\boldsymbol{k}_0 \tag{1.1}$$

is satisfied, where $\omega(\boldsymbol{k})$ is the frequency of a plane wave with a two-dimensional wavenumber $\boldsymbol{k}$ and is obtained from the linear dispersion relation. The main wave has a wavenumber $\boldsymbol{k}_0 = (k_0, 0)$ while $\boldsymbol{k}_1$ and $\boldsymbol{k}_2$ denote the wavenumbers of the perturbation. N is a positive integer. This resonance condition is described in further details in the excellent review article by Phillips (1981).

For interfacial waves this angular frequency is given by

$$\omega(\boldsymbol{k}) = \left\{\frac{(\rho_2-\rho_1)\,g|\boldsymbol{k}|}{\rho_1 \coth|\boldsymbol{k}|d_1+\rho_2\coth|\boldsymbol{k}|d_2}\right\}^{\frac{1}{2}}, \tag{1.2}$$

† Now at School of Engineering, University of Exeter, North Park Road, Exeter EX4 4QF, UK.

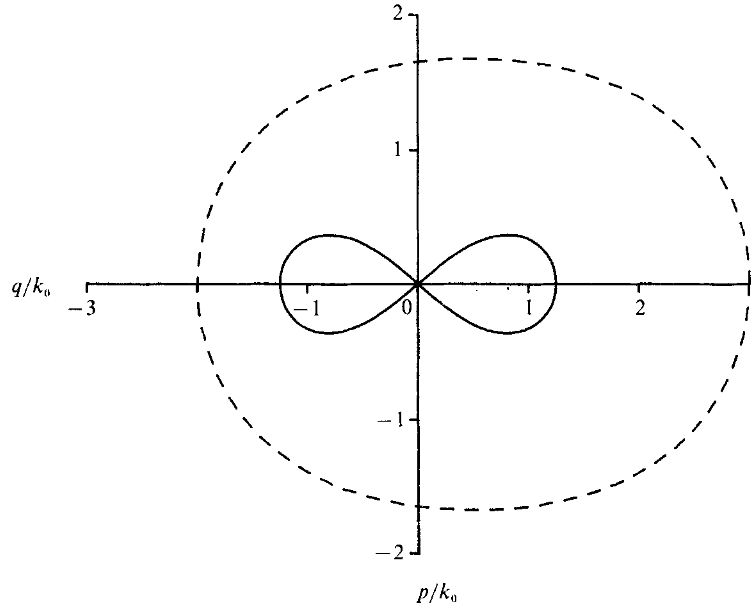

FIGURE 1. Solution of equation (1.1) for $\boldsymbol{p} = (p, q)$ showing resonance curves. Quartet resonance, $N = 2$, (continuous line); quintet resonance, $N = 3$, (dashed).

where $\rho_1(\rho_2)$ is the density of the upper (lower) fluid, $d_1(d_2)$ is the depth of the upper (lower) fluid and g is the gravitational acceleration. For the case of surface waves, where $\rho_1 = 0$, this reduces to

$$\omega(\boldsymbol{k}) = \{g|\boldsymbol{k}| \tanh |\boldsymbol{k}|d_2\}^{\frac{1}{2}}.$$

The case when $N = 1$, the triad resonance, does not exist for surface or interfacial waves in the absence of shear. This was shown by Phillips (1960) for the case of surface waves, while Pullin & Grimshaw (1985) extended this argument to include interfacial waves. In contrast, Craik (1968) and a later paper by Pullin & Grimshaw (1986), showed the existence of triad resonances if a sufficiently strong current shear was introduced.

The case when $N = 2$, the quartet resonance, can be found by setting $\boldsymbol{k}_1 = \boldsymbol{k}_0 + \boldsymbol{p}$ and $\boldsymbol{k}_2 = \boldsymbol{k}_0 - \boldsymbol{p}$, where $\boldsymbol{p} = (p, q)$ is termed the perturbation wavenumber. The solution curve for (1.1) of p against q can be seen in figure 1 and takes the form of a 'figure of 8'. This was first found by Phillips (1960) for the case of surface waves.

The quintet resonant curve, $N = 3$, can also be found by setting $\boldsymbol{k}_1 = \boldsymbol{k}_0 + \boldsymbol{p}$ and $\boldsymbol{k}_2 = 2\boldsymbol{k}_0 - \boldsymbol{p}$ and is plotted in figure 1. This curve is symmetric about $p = 0.5$.

Equation (1.1) gives only the perturbation wavenumbers where resonances can occur for infinitesimal wave steepnesses and says nothing about the growth rates. Three different techniques have been used to model the evolution of this wave system and hence calculate the growth rates, these being a numerical method based on a spectral expansion, the use of the Zakharov equation for the case of surface waves, or the use of a nonlinear Schrödinger equation. The nonlinear Schrödinger equation describing three-dimensional, finite-depth surface waves was derived by Davey & Stewartson (1974) using a multiple scale technique. It was assumed that both the wave steepness and the spectral bandwidth of the solution are small and hence a coupled pair of equations describing the amplitude and the mean flow was derived, the Davey–Stewartson equations. Upon assuming that the modulation of the amplitude and mean flow is of the form of a plane periodic wave a nonlinear Schrödinger equation was then obtained. A subsequent stability analysis was then done on a periodic wave which gave the growth rates for the quartet resonance, restricted to small perturbation wavenumbers.

The Zakharov equation for surface waves was first derived by Zakharov (1968) for the infinite-depth case and later extended to the finite-depth case, in Zakharov & Kharitonov (1970). The Zakharov equation is superior to the nonlinear Schrödinger equation in that the perturbation wavenumber is not assumed to be small and hence the resonant instability can be investigated for all perturbation wavenumbers. An extensive stability analysis was not given in these papers but was first done by Crawford *et al.* (1981) who found a restabilization of the quartet resonance for large wave steepnesses, in agreement with previous numerical work by Longuet-Higgins (1978*a*, *b*). Stiassnie & Shemer (1984) extended the finite-depth Zakharov equation to fourth order, such that both quartet and quintet resonances could be investigated as quartet resonances are described by third-order effects and the quintet by fourth.

In the first of a series of papers Grimshaw & Pullin (1985) derived the nonlinear Schrödinger equation, coupled to a wave-induced mean-flow equation, for interfacial waves between fluids of finite depths and a given ratio of fluid densities. These equations are analogous to the Davey–Stewartson equations for surface waves. A stability analysis was then done which showed that for infinite depths the perturbation wavenumber for maximum growth rate was two-dimensional, i.e. parallel to the wavenumber of the main wave, and with a wavenumber close to zero. For finite depths this wavenumber of maximum growth rate was generally three-dimensional as the region of small-perturbation wavenumber restabilized. Yuen (1984) used a numerical technique, similar to that of McLean (1982*a*,*b*) for surface waves, to investigate the stability of interfacial waves in the presence of a current jump across the interface. Quartet and quintet resonances were found, along with a Kelvin–Helmholtz instability when the current jump was present. In the second paper by Pullin & Grimshaw (1985) a numerical technique was also used to examine the stability of a finite-amplitude interfacial wave in the Boussinesq limit, with the lower fluid infinitely deep. For small wave steepnesses it was found that the instabilities were dominated by resonant quartets, with higher-order effects not as important. For larger wave steepnesses these were swamped by a Kelvin–Helmholtz instability. No restabilization of the quartet resonance was found in the wave steepnesses investigated, that is below the Kelvin–Helmholtz threshold. As with surface waves, McLean (1982*a*,*b*), it was found that the growth rates of these resonant instabilities behaved as the wave steepness raised to the power of N, where N is defined as in (1.1). In a third paper, Pullin & Grimshaw (1986), the effects of a basic current shear were introduced.

In this paper an amplitude equation for interfacial waves, similar to the Zakharov equation for surface waves, is derived in §2. No assumption is made on the depths or fluid densities, unlike the above numerical methods. From this a nonlinear Schrödinger equation, coupled to a wave-induced mean-flow equation, is found in §3 under the assumption that the solution is a periodic wave with a long wavelength modulation. Using this Zakharov equation a linear stability analysis is then carried out on a steady, periodic solution. In agreement with these numerical accounts it is found that for small wave steepnesses the instabilities are due to quartet resonances but for large wave steepnesses, and small values of the Boussinesq parameter, another instability is found which is shown to be a Kelvin–Helmholtz instability induced by the main wave.

2. Derivation of the Zakharov equation for the case of interfacial waves

Consider a two-layer fluid with densities ρ_1 and ρ_2, such that $\rho_1 < \rho_2$, where the subscripts 1 and 2 refer to the fluid properties of the upper and lower fluids respectively. The fluid is bounded by horizontal planes at $z = d_1$ and $z = -d_2$ and the interface is at $z = \eta(\boldsymbol{x}, t)$, where $\boldsymbol{x} = (x, y)$. Gravity acts in the negative z-direction. The flow is considered to be irrotational and described by the velocity potentials $\phi_j(\boldsymbol{x}, z, t), (j = 1, 2)$, where the flow field is given by $\boldsymbol{v}_j = (u_j, v_j, w_j) = \boldsymbol{\nabla}\phi_j$.

The two kinematic boundary conditions at the interface are given by

$$\eta_t + \boldsymbol{\nabla}_x \phi_j \cdot \boldsymbol{\nabla}_x \eta = \phi_{j,z} \quad \text{on} \quad z = \eta \quad (j = 1, 2), \tag{2.1}$$

where $\boldsymbol{\nabla}_x = (\partial/\partial x, \partial/\partial y)$ and $\phi_{j,z} = (\partial/\partial z)\phi_j$ etc. The dynamic condition is given by the restriction that the pressure is continuous across the interface, giving

$$\sum_j (-1)^j \rho_j \{\phi_{j,t} + \tfrac{1}{2}(\boldsymbol{\nabla}\phi_j)^2 + g\eta\} = 0 \quad \text{on} \quad z = \eta, \tag{2.2}$$

from Bernoulli's theorem.

As the fluids are assumed to be incompressible then

$$\nabla^2 \phi_j = 0 \tag{2.3}$$

and the conditions at the boundaries are

$$\phi_{j,z} = 0 \quad \text{at} \quad z = d_1, -d_2. \tag{2.4}$$

Following the method outlined by Yuen & Lake (1982) for the derivation of the Zakharov equation for surface waves, we define the velocity potential at the interface to be $\phi_j^s(\boldsymbol{x}, t)$, viz.

$$\phi_j^s(\boldsymbol{x}, t) = \phi_j(\boldsymbol{x}, \eta(\boldsymbol{x}, t), t).$$

This gives the kinematic boundary conditions at the interface to be

$$\eta_t + \boldsymbol{\nabla}_x \phi_j^s \cdot \boldsymbol{\nabla}_x \eta - \phi_{j,z}(1 + (\boldsymbol{\nabla}_x \eta)^2) = 0 \quad (j = 1, 2) \tag{2.5}$$

and the dynamic condition becomes

$$\sum_j (-1)^j \rho_j \{\phi_{j,t}^s + \tfrac{1}{2}(\boldsymbol{\nabla}_x \phi_j^s)^2 - \tfrac{1}{2}\phi_{j,z}^2(1 + (\boldsymbol{\nabla}_x \eta)^2) + g\eta)\} = 0, \tag{2.6}$$

with $\phi_{j,z}$ evaluated at $z = \eta$.

An approximation to the Fourier transform of these boundary conditions can be found under the assumption that the disturbance at the interface is small, and hence can be truncated to third order in wave steepness. The major difficulty is finding the Fourier transform of $\phi_{j,z}(\boldsymbol{x}, \eta, t)$.

Define the Fourier transform of the velocity potential as

$$\hat{\phi}_j(\boldsymbol{k}, z, t) = F\{\phi_j(\boldsymbol{x}, z, t)\} = \frac{1}{2\pi}\int_{-\infty}^{\infty} \phi_j(\boldsymbol{x}, z, t)\, \mathrm{e}^{-\mathrm{i}\boldsymbol{k}\boldsymbol{x}}\, \mathrm{d}\boldsymbol{x}, \tag{2.7}$$

where $F\{\ \}$ denotes the Fourier transform operation. Upon setting

$$\phi_j(\boldsymbol{x}, z, t) = \frac{1}{2\pi}\int_{-\infty}^{\infty} \hat{\Phi}_j(\boldsymbol{k}, t) \cosh(|\boldsymbol{k}|(z + (-1)^j d_j))\, \mathrm{e}^{\mathrm{i}\boldsymbol{k}\boldsymbol{x}}\, \mathrm{d}\boldsymbol{k}, \tag{2.8}$$

which satisfies (2.3) and (2.4), and expanding to second order in $\eta(\boldsymbol{x},t)$ one obtains

$$\begin{aligned}\phi_j^s(\boldsymbol{x}) = \phi_j(\boldsymbol{x},\eta) = &\frac{1}{2\pi}\int_{-\infty}^{\infty} \hat{\Phi}_j(\boldsymbol{k})\, c_j(k)\, e^{i\boldsymbol{k}\boldsymbol{x}}\, d\boldsymbol{k} \\ &+\frac{(-1)^j}{(2\pi)^2}\int_{-\infty}^{\infty}\int_{-\infty}^{\infty} \hat{\Phi}_j(\boldsymbol{k})\, |\boldsymbol{k}| s_j(\boldsymbol{k})\, \hat{\eta}(\boldsymbol{k}_1)\, e^{i(\boldsymbol{k}+\boldsymbol{k}_1)\boldsymbol{x}}\, d\boldsymbol{k}\, d\boldsymbol{k}_1 \\ &+\frac{1}{(2\pi)^3}\int_{-\infty}^{\infty}\int_{-\infty}^{\infty}\int_{-\infty}^{\infty} \tfrac{1}{2}\hat{\Phi}_j(\boldsymbol{k})\, c_j(\boldsymbol{k})\, \boldsymbol{k}^2 \hat{\eta}(\boldsymbol{k}_1)\, \hat{\eta}(\boldsymbol{k}_2)\, e^{i(\boldsymbol{k}+\boldsymbol{k}_1+\boldsymbol{k}_2)\boldsymbol{x}}\, d\boldsymbol{k}\, d\boldsymbol{k}_1\, d\boldsymbol{k}_2 \\ &+\dots, \end{aligned} \tag{2.9}$$

where $c_j(\boldsymbol{k}) = \cosh(|\boldsymbol{k}|d_j), s_j(\boldsymbol{k}) = \sinh(|\boldsymbol{k}|d_j)$ and $\hat{\eta}(\boldsymbol{k})$ is the Fourier transform of $\eta(\boldsymbol{x},t)$. The time dependence has been dropped in the notation but is still implied. The Fourier transform of the above equation can be taken, from which $\hat{\Phi}_j(\boldsymbol{k},t)$ can be found to third order using an iterative method, and hence the Fourier transform of $\phi_{j,z}(\boldsymbol{x},\eta,t)$ from (2.8). The Fourier transform of the kinematic boundary condition is then found to be

$$\begin{aligned}&\hat{\eta}_t(\boldsymbol{k}) - (-1)^j |\boldsymbol{k}| tn_j(\boldsymbol{k})\, \hat{\phi}_j^s(\boldsymbol{k}) \\ &+\frac{1}{2\pi}\int_{-\infty}^{\infty}\int_{-\infty}^{\infty} \hat{\phi}_j^s(\boldsymbol{k}_1)\, \alpha_j(\boldsymbol{k}, -\boldsymbol{k}_1, \boldsymbol{k}_2)\, \hat{\eta}(\boldsymbol{k}_2)\, \delta(\boldsymbol{k}-\boldsymbol{k}_1-\boldsymbol{k}_2)\, d\boldsymbol{k}_1\, d\boldsymbol{k}_2 \\ &+\frac{(-1)^j}{(2\pi)^2}\int_{-\infty}^{\infty}\int_{-\infty}^{\infty}\int_{-\infty}^{\infty} \hat{\phi}_j^s(\boldsymbol{k}_1)\, \beta_j(-\boldsymbol{k}, \boldsymbol{k}_1, \boldsymbol{k}_2, \boldsymbol{k}_3)\, \eta(\boldsymbol{k}_2)\, \eta(\boldsymbol{k}_3) \\ &\times \delta(\boldsymbol{k}-\boldsymbol{k}_1-\boldsymbol{k}_2-\boldsymbol{k}_3)\, d\boldsymbol{k}_1\, d\boldsymbol{k}_2\, d\boldsymbol{k}_3 \\ &+\dots = 0 \quad (j = 1, 2), \end{aligned} \tag{2.10}$$

where

$$\alpha_j(\boldsymbol{k},\boldsymbol{k}_1) = |\boldsymbol{k}|\,|\boldsymbol{k}_1| tn_j(\boldsymbol{k})\, tn_j(\boldsymbol{k}_1) + \boldsymbol{k}\cdot\boldsymbol{k}_1,$$

$$\begin{aligned}\beta_j(\boldsymbol{k},\boldsymbol{k}_1,\boldsymbol{k}_2,\boldsymbol{k}_3) = \tfrac{1}{4}|\boldsymbol{k}|\,|\boldsymbol{k}_1|(&2|\boldsymbol{k}| tn_j(\boldsymbol{k}_1) + 2|\boldsymbol{k}_1| tn_j(\boldsymbol{k}) - tn_j(\boldsymbol{k})\, tn_j(\boldsymbol{k}_1)\, [|\boldsymbol{k}_1+\boldsymbol{k}_3| tn_j(\boldsymbol{k}_1+\boldsymbol{k}_3) \\ &+ |\boldsymbol{k}_1+\boldsymbol{k}_2| tn_j(\boldsymbol{k}_1+\boldsymbol{k}_2) + |\boldsymbol{k}+\boldsymbol{k}_2| tn_j(\boldsymbol{k}+\boldsymbol{k}_2) + |\boldsymbol{k}+\boldsymbol{k}_3| tn_j(\boldsymbol{k}+\boldsymbol{k}_3)]).\end{aligned}$$

and

$$tn_j(\boldsymbol{k}) = \tanh(|\boldsymbol{k}|d_j).$$

Similarly, the Fourier transform of the dynamic condition becomes

$$\rho_1 F_1(\boldsymbol{k},\boldsymbol{k}_1,\boldsymbol{k}_2,\boldsymbol{k}_3) - \rho_2 F_2(\boldsymbol{k},\boldsymbol{k}_1,\boldsymbol{k}_2,\boldsymbol{k}_3) = 0, \tag{2.11}$$

where

$$\begin{aligned}F_j(\boldsymbol{k},\boldsymbol{k}_1,\boldsymbol{k}_2,\boldsymbol{k}_3) = &\hat{\phi}_{j,t}^s(\boldsymbol{k}) + g\hat{\eta}(\boldsymbol{k}) \\ &-\frac{1}{2\pi}\int_{-\infty}^{\infty}\int_{-\infty}^{\infty} \tfrac{1}{2}\hat{\phi}_j^s(\boldsymbol{k}_1)\, \hat{\phi}_j^s(\boldsymbol{k}_2)\, \alpha_j(\boldsymbol{k}_1,\boldsymbol{k}_2,\boldsymbol{k})\, \delta(\boldsymbol{k}-\boldsymbol{k}_1-\boldsymbol{k}_2)\, d\boldsymbol{k}_1\, d\boldsymbol{k}_2 \\ &-\frac{(-1)^j}{(2\pi)^2}\int_{-\infty}^{\infty}\int_{-\infty}^{\infty}\int_{-\infty}^{\infty} \hat{\phi}_j^s(\boldsymbol{k}_1)\, \hat{\phi}_j^s(\boldsymbol{k}_1)\, \beta_j(\boldsymbol{k}_1,\boldsymbol{k}_2,\boldsymbol{k}_3,-\boldsymbol{k})\, \hat{\eta}(\boldsymbol{k}_3) \\ &\times \delta(\boldsymbol{k}-\boldsymbol{k}_1-\boldsymbol{k}_2-\boldsymbol{k}_3)\, d\boldsymbol{k}_1\, d\boldsymbol{k}_2\, d\boldsymbol{k}_3 \\ &+\dots. \end{aligned} \tag{2.12}$$

These expressions can further be reduced with the substitutions

$$\Psi(\boldsymbol{k}) = tn_1(\boldsymbol{k})\, \hat{\phi}_1^s(\boldsymbol{k}) + tn_2(\boldsymbol{k})\, \hat{\phi}_2^s(\boldsymbol{k})$$

and

$$\rho\hat{\phi}^s(\boldsymbol{k}) = \rho_2 \hat{\phi}_2^s(\boldsymbol{k}) - \rho_1 \hat{\phi}_1^s(\boldsymbol{k}),$$

where $\rho = \rho_1 + \rho_2$ and we let $\alpha = (\rho_2 - \rho_1)/\rho$. The term α is called the Boussinesq parameter. For surface waves it has a value of unity but if the densities of the fluids are nearly equal, the Boussinesq limit, it is approximately zero. By subtracting (2.10) with $j = 1$, from itself with $j = 2$, then $\Psi(\boldsymbol{k})$ can be found using an iterative technique, as it is a second-order quantity. This gives $\psi(\boldsymbol{k})$, to third order, to be

$$|\boldsymbol{k}|\Psi(\boldsymbol{k}) = \frac{1}{2\pi}\int_{-\infty}^{\infty}\int_{-\infty}^{\infty} \hat{\phi}^{s}(\boldsymbol{k})\,\hat{\Psi}_2(\boldsymbol{k},\boldsymbol{k}_1,\boldsymbol{k}_2)\,\hat{\eta}(\boldsymbol{k}_2)\,\delta(\boldsymbol{k}-\boldsymbol{k}_1-\boldsymbol{k}_2)\,\mathrm{d}\boldsymbol{k}_1\,\mathrm{d}\boldsymbol{k}_2$$
$$+\frac{1}{(2\pi)^2}\int_{-\infty}^{\infty}\int_{-\infty}^{\infty}\int_{-\infty}^{\infty} \hat{\phi}^{s}(\boldsymbol{k}_1)\,\hat{\Psi}_3(\boldsymbol{k},\boldsymbol{k}_1,\boldsymbol{k}_2,\boldsymbol{k}_3)\,\hat{\eta}(\boldsymbol{k}_2)\,\hat{\eta}(\boldsymbol{k}_3)\,\delta(\boldsymbol{k}-\boldsymbol{k}_1-\boldsymbol{k}_2-\boldsymbol{k}_3)$$
$$\times\,\mathrm{d}\boldsymbol{k}_1\,\mathrm{d}\boldsymbol{k}_2\,\mathrm{d}\boldsymbol{k}_3 + \dots . \tag{2.13}$$

The terms $\hat{\Psi}_j$ are not written here owing to their complexity. The interfacial boundary conditions can then be reduced to a system in terms of $\hat{\eta}$ and $\hat{\phi}^{s}$ alone:

$$\hat{\eta}_t(\boldsymbol{k}) - |\boldsymbol{k}|\lambda(\boldsymbol{k})\,\hat{\phi}^{s}(\boldsymbol{k})$$
$$+4\int_{-\infty}^{\infty}\int_{-\infty}^{\infty} \hat{\phi}^{s}(\boldsymbol{k}_1)\left(\frac{2\omega(\boldsymbol{k})\,\omega(\boldsymbol{k}_1)}{\alpha g\,\omega(\boldsymbol{k}_2)}\right)^{\frac{1}{2}} V(\boldsymbol{k},-\boldsymbol{k}_1,\boldsymbol{k}_2)\,\hat{\eta}(\boldsymbol{k}_2)\,\delta(\boldsymbol{k}-\boldsymbol{k}_1-\boldsymbol{k}_2)\,\mathrm{d}\boldsymbol{k}_1\,\mathrm{d}\boldsymbol{k}_2\,\mathrm{d}\boldsymbol{k}_3$$
$$+4\int_{-\infty}^{\infty}\int_{-\infty}^{\infty}\int_{-\infty}^{\infty} \hat{\phi}^{s}(\boldsymbol{k}_1)\left(\frac{\omega(\boldsymbol{k})\,\omega(\boldsymbol{k}_1)}{\omega(\boldsymbol{k}_2)\,\omega(\boldsymbol{k}_3)}\right)^{\frac{1}{2}}\{W(-\boldsymbol{k},\boldsymbol{k}_1,\boldsymbol{k}_2,\boldsymbol{k}_3)+\tfrac{1}{4}(1-\alpha^2)\,Y(\boldsymbol{k},\boldsymbol{k}_1,\boldsymbol{k}_2,\boldsymbol{k}_3)\}$$
$$\times\,\hat{\eta}(\boldsymbol{k}_2)\,\hat{\eta}(\boldsymbol{k}_3)\,\delta(\boldsymbol{k}-\boldsymbol{k}_1-\boldsymbol{k}_2-\boldsymbol{k}_3)\,\mathrm{d}\boldsymbol{k}_1\,\mathrm{d}\boldsymbol{k}_2\,\mathrm{d}\boldsymbol{k}_3 + \dots = 0 \tag{2.14}$$

and

$$\hat{\phi}^{s}_t(\boldsymbol{k}) + \alpha g\,\hat{\eta}(\boldsymbol{k})$$
$$-2\int_{-\infty}^{\infty}\int_{-\infty}^{\infty} \hat{\phi}^{s}(\boldsymbol{k}_1)\left(\frac{2\omega(\boldsymbol{k}_1)\,\omega(\boldsymbol{k}_2)}{g\alpha\,\omega(\boldsymbol{k})}\right)^{\frac{1}{2}} V(\boldsymbol{k}_1,\boldsymbol{k}_2,\boldsymbol{k})\,\hat{\phi}^{s}(\boldsymbol{k}_2)\,\delta(\boldsymbol{k}-\boldsymbol{k}_1-\boldsymbol{k}_2)\,\mathrm{d}\boldsymbol{k}_1\,\mathrm{d}\boldsymbol{k}_2$$
$$-4\int_{-\infty}^{\infty}\int_{-\infty}^{\infty}\int_{-\infty}^{\infty} \hat{\phi}^{s}(\boldsymbol{k}_1)\left(\frac{\omega(\boldsymbol{k}_1)\,\omega(\boldsymbol{k}_2)}{\omega(\boldsymbol{k})\,\omega(\boldsymbol{k}_3)}\right)^{\frac{1}{2}}\{W(\boldsymbol{k}_1,\boldsymbol{k}_2,\boldsymbol{k}_3,-\boldsymbol{k})+\tfrac{1}{4}(1-\alpha^2)$$
$$\times\,Y(-\boldsymbol{k}_2,\boldsymbol{k}_1,\boldsymbol{k},\boldsymbol{k}_3)\}\,\hat{\phi}^{s}(\boldsymbol{k}_2)\,\hat{\eta}(\boldsymbol{k}_3)\,\delta(\boldsymbol{k}-\boldsymbol{k}_1-\boldsymbol{k}_2-\boldsymbol{k}_3)\,\mathrm{d}\boldsymbol{k}_1\,\mathrm{d}\boldsymbol{k}_2\,\mathrm{d}\boldsymbol{k}_3$$
$$+ \dots = 0, \tag{2.15}$$

where $V(\boldsymbol{k},\boldsymbol{k}_1,\boldsymbol{k}_2)$, $W(\boldsymbol{k},\boldsymbol{k}_1,\boldsymbol{k}_2,\boldsymbol{k}_3)$ and $Y(\boldsymbol{k},\boldsymbol{k}_1,\boldsymbol{k}_2,\boldsymbol{k}_3)$ are defined in Appendix A. The subsequent analysis parallels closely that of the derivation for surface waves. Defining

$$b(\boldsymbol{k},t) = \left\{\frac{\alpha g}{2\omega(\boldsymbol{k})}\right\}^{\frac{1}{2}}\hat{\eta}(\boldsymbol{k}) + \mathrm{i}\left\{\frac{\omega(\boldsymbol{k})}{2\alpha g}\right\}^{\frac{1}{2}}\hat{\phi}^{s}(\boldsymbol{k}), \tag{2.16}$$

then

$$\hat{\eta}(\boldsymbol{k}) = \left(\frac{|\boldsymbol{k}|\lambda(\boldsymbol{k})}{2\omega(\boldsymbol{k})}\right)^{\frac{1}{2}}(b(\boldsymbol{k},t)+b^{*}(-\boldsymbol{k},t))$$

etc. as $\hat{\eta}(\boldsymbol{k})$ is a Fourier transform of a real function and hence $\hat{\eta}^{*}(-\boldsymbol{k}) = \hat{\eta}(\boldsymbol{k})$. The asterisk superscript implies the complex conjugate, with the functions $\lambda(\boldsymbol{k})$ and $\omega(\boldsymbol{k})$ given by

$$\lambda(\boldsymbol{k}) = \frac{\rho}{\rho_1/tn_1(\boldsymbol{k})+\rho_2/tn_2(\boldsymbol{k})}; \quad \omega(\boldsymbol{k}) = (\alpha g|\boldsymbol{k}|\lambda(\boldsymbol{k}))^{\frac{1}{2}}, \tag{2.17}$$

the latter being the linear dispersion relation for travelling waves along the interface.

Combining (2.14), (2.15) and (2.16) the interfacial boundary conditions reduce to the single equation

$$
\begin{aligned}
& b_t(\boldsymbol{k})+\mathrm{i}\omega(\boldsymbol{k})\, b(\boldsymbol{k})+\mathrm{i}\int_{-\infty}^{\infty}\int_{-\infty}^{\infty} v^{(1)}(\boldsymbol{k},\boldsymbol{k}_1,\boldsymbol{k}_2)\,\delta(\boldsymbol{k}-\boldsymbol{k}_1-\boldsymbol{k}_2)\, b(\boldsymbol{k}_1)\, b(\boldsymbol{k}_2)\,\mathrm{d}\boldsymbol{k}_1\,\mathrm{d}\boldsymbol{k}_2 \\
& \quad +\mathrm{i}\int_{-\infty}^{\infty}\int_{-\infty}^{\infty} v^{(2)}(\boldsymbol{k},\boldsymbol{k}_1,\boldsymbol{k}_2)\,\delta(\boldsymbol{k}+\boldsymbol{k}_1-\boldsymbol{k}_2)\, b^*(\boldsymbol{k}_1)\, b(\boldsymbol{k}_2)\,\mathrm{d}\boldsymbol{k}_1\,\mathrm{d}\boldsymbol{k}_2 \\
& \quad +\mathrm{i}\int_{-\infty}^{\infty}\int_{-\infty}^{\infty} v^{(3)}(\boldsymbol{k},\boldsymbol{k}_1,\boldsymbol{k}_2)\,\delta(\boldsymbol{k}+\boldsymbol{k}_1+\boldsymbol{k}_2)\, b^*(\boldsymbol{k}_1)\, b^*(\boldsymbol{k}_2)\,\mathrm{d}\boldsymbol{k}_1\,\mathrm{d}\boldsymbol{k}_2 \\
& \quad +\mathrm{i}\int_{-\infty}^{\infty}\int_{-\infty}^{\infty}\int_{-\infty}^{\infty} [w^{(1)}(\boldsymbol{k},\boldsymbol{k}_1,\boldsymbol{k}_2,\boldsymbol{k}_3)+\tfrac{1}{4}(1-\alpha^2)\, y^{(1)}(\boldsymbol{k},\boldsymbol{k}_1,\boldsymbol{k}_2,\boldsymbol{k}_3)]\,\delta(\boldsymbol{k}-\boldsymbol{k}_1-\boldsymbol{k}_2-\boldsymbol{k}_3) \\
& \qquad\qquad \times b(\boldsymbol{k}_1)\, b(\boldsymbol{k}_2)\, b(\boldsymbol{k}_3)\,\mathrm{d}\boldsymbol{k}_1\,\mathrm{d}\boldsymbol{k}_2\,\mathrm{d}\boldsymbol{k}_3 \\
& \quad +\mathrm{i}\int_{-\infty}^{\infty}\int_{-\infty}^{\infty}\int_{-\infty}^{\infty} [w^{(2)}(\boldsymbol{k},\boldsymbol{k}_1,\boldsymbol{k}_2,\boldsymbol{k}_3)+\tfrac{1}{4}(1-\alpha^2)\, y^{(2)}(\boldsymbol{k},\boldsymbol{k}_1,\boldsymbol{k}_2,\boldsymbol{k}_3)]\,\delta(\boldsymbol{k}+\boldsymbol{k}_1-\boldsymbol{k}_2-\boldsymbol{k}_3) \\
& \qquad\qquad \times b^*(\boldsymbol{k}_1)\, b(\boldsymbol{k}_2)\, b(\boldsymbol{k}_3)\,\mathrm{d}\boldsymbol{k}_1\,\mathrm{d}\boldsymbol{k}_2\,\mathrm{d}\boldsymbol{k}_3 \\
& \quad +\mathrm{i}\int_{-\infty}^{\infty}\int_{-\infty}^{\infty}\int_{-\infty}^{\infty} [w^{(3)}(\boldsymbol{k},\boldsymbol{k}_1,\boldsymbol{k}_2,\boldsymbol{k}_3)+\tfrac{1}{4}(1-\alpha^2)\, y^{(3)}(\boldsymbol{k},\boldsymbol{k}_1,\boldsymbol{k}_2,\boldsymbol{k}_3)]\,\delta(\boldsymbol{k}+\boldsymbol{k}_1+\boldsymbol{k}_2-\boldsymbol{k}_3) \\
& \qquad\qquad \times b^*(\boldsymbol{k}_1)\, b^*(\boldsymbol{k}_2)\, b(\boldsymbol{k}_3)\,\mathrm{d}\boldsymbol{k}_1\,\mathrm{d}\boldsymbol{k}_2\,\mathrm{d}\boldsymbol{k}_3 \\
& \quad +\mathrm{i}\int_{-\infty}^{\infty}\int_{-\infty}^{\infty}\int_{-\infty}^{\infty} [w^{(4)}(\boldsymbol{k},\boldsymbol{k}_1,\boldsymbol{k}_2,\boldsymbol{k}_3)+\tfrac{1}{4}(1-\alpha^2)\, y^{(4)}(\boldsymbol{k},\boldsymbol{k}_1,\boldsymbol{k}_2,\boldsymbol{k}_3)]\,\delta(\boldsymbol{k}+\boldsymbol{k}_1+\boldsymbol{k}_2+\boldsymbol{k}_3) \\
& \qquad\qquad \times b^*(\boldsymbol{k}_1)\, b^*(\boldsymbol{k}_2)\, b^*(\boldsymbol{k}_3)\,\mathrm{d}\boldsymbol{k}_1\,\mathrm{d}\boldsymbol{k}_2\,\mathrm{d}\boldsymbol{k}_3 \\
& \quad +\ldots = 0,
\end{aligned} \tag{2.18}
$$

where the coefficients $v^{(j)}$, $y^{(2)}$ and $w^{(2)}$ are defined in Appendix A. The solution to the linearized version of (2.18) is the simple periodic wave $b(k) = b_0 \exp(\mathrm{i}\omega(\boldsymbol{k})\,t)$, b_0 being a contant, whereas the integral terms give the second- and third-order nonlinear corrections.

As triad resonances do not exist the evolution of the wave at small steepnesses is governed by the quartet resonance. The evolution timescale is then of the order of the square of the reciprocal of the wave steepnesses. This permits us to set

$$
b(\boldsymbol{k},t) = [\epsilon B(\boldsymbol{k},\tau)+\epsilon^2 B'(\boldsymbol{k},t)]\,\mathrm{e}^{-\mathrm{i}\omega(\boldsymbol{k})\,t}, \tag{2.19}
$$

where $\tau = \epsilon^2 t$ and ϵ is a measure of the nonlinearity. The linear component B varies on the slow timescale τ. Upon substitution of (2.19) into (2.18), $B'(\boldsymbol{k},t)$ can be found from the second-order equations by direct integration with respect to time. This term contains the nonlinear corrections such as the wave-induced mean flow and the first harmonic. After the substitution of B' back into (2.18) one obtains

$$
\begin{aligned}
\mathrm{i}B_\tau(\boldsymbol{k}) = & \int_{-\infty}^{\infty}\int_{-\infty}^{\infty}\int_{-\infty}^{\infty} T_1(\boldsymbol{k},\boldsymbol{k}_1,\boldsymbol{k}_2,\boldsymbol{k}_3)\,\delta(\boldsymbol{k}-\boldsymbol{k}_1-\boldsymbol{k}_2-\boldsymbol{k}_3)\, B(\boldsymbol{k}_1)\, B(\boldsymbol{k}_2)\, B(\boldsymbol{k}_3) \\
& \qquad \mathrm{e}^{\mathrm{i}(\omega(\boldsymbol{k})-\omega(\boldsymbol{k}_1)-\omega(\boldsymbol{k}_2)-\omega(\boldsymbol{k}_3))\,t}\,\mathrm{d}\boldsymbol{k}_1\,\mathrm{d}\boldsymbol{k}_2\,\mathrm{d}\boldsymbol{k}_3 \\
& +\int_{-\infty}^{\infty}\int_{-\infty}^{\infty}\int_{-\infty}^{\infty} T_2(\boldsymbol{k},\boldsymbol{k}_1,\boldsymbol{k}_2,\boldsymbol{k}_3)\,\delta(\boldsymbol{k}+\boldsymbol{k}_1-\boldsymbol{k}_2-\boldsymbol{k}_3)\, B^*(\boldsymbol{k}_1) B(\boldsymbol{k}_2) B(\boldsymbol{k}_3) \\
& \qquad \mathrm{e}^{\mathrm{i}(\omega(\boldsymbol{k})+\omega(\boldsymbol{k}_1)-\omega(\boldsymbol{k}_2)-\omega(\boldsymbol{k}_3))\,t}\,\mathrm{d}\boldsymbol{k}_1\,\mathrm{d}\boldsymbol{k}_2\,\mathrm{d}\boldsymbol{k}_3 \\
& +\int_{-\infty}^{\infty}\int_{-\infty}^{\infty}\int_{-\infty}^{\infty} T_3(\boldsymbol{k},\boldsymbol{k}_1,\boldsymbol{k}_2,\boldsymbol{k}_3)\,\delta(\boldsymbol{k}+\boldsymbol{k}_1+\boldsymbol{k}_2-\boldsymbol{k}_3)\, B^*(\boldsymbol{k}_1) B^*(\boldsymbol{k}_2) B(\boldsymbol{k}_3) \\
& \qquad \mathrm{e}^{\mathrm{i}(\omega(\boldsymbol{k})+\omega(\boldsymbol{k}_1)+\omega(\boldsymbol{k}_2)-\omega(\boldsymbol{k}_3))\,t}\,\mathrm{d}\boldsymbol{k}_1\,\mathrm{d}\boldsymbol{k}_2\,\mathrm{d}\boldsymbol{k}_3
\end{aligned}
$$

$$+\int_{-\infty}^{\infty}\int_{-\infty}^{\infty}\int_{-\infty}^{\infty} T_4(\boldsymbol{k},\boldsymbol{k}_1,\boldsymbol{k}_2,\boldsymbol{k}_3)\,\delta(\boldsymbol{k}+\boldsymbol{k}_1+\boldsymbol{k}_2+\boldsymbol{k}_3)B^*(\boldsymbol{k}_1)B^*(\boldsymbol{k}_2)B^*(\boldsymbol{k}_3)\, \mathrm{e}^{\mathrm{i}(\omega(\boldsymbol{k})+\omega(\boldsymbol{k}_1)+\omega(\boldsymbol{k}_2)+\omega(\boldsymbol{k}_3))t}\,\mathrm{d}\boldsymbol{k}_1\,\mathrm{d}\boldsymbol{k}_2\,\mathrm{d}\boldsymbol{k}_3 + \dots \quad (2.20)$$

The Zakharov equation is found by excluding the terms with a fast time variation, as these would be smaller upon integrating with time than the terms with a slow time variation. This leaves only the second nonlinear term of (2.20) and only near the region of the quartet resonance given by (1.1). Away from this region all the nonlinear terms are of equal importance as is discussed in Appendix C.

The Zakharov equation is then

$$\mathrm{i}B_t(\boldsymbol{k}) = \int_{-\infty}^{\infty}\int_{-\infty}^{\infty}\int_{-\infty}^{\infty} T(\boldsymbol{k},\boldsymbol{k}_1,\boldsymbol{k}_2,\boldsymbol{k}_3)\,\mathrm{e}^{\mathrm{i}(\omega(\boldsymbol{k})+\omega(\boldsymbol{k}_1)-\omega(\boldsymbol{k}_2)-\omega(\boldsymbol{k}_3))t} \times\delta(\boldsymbol{k}+\boldsymbol{k}_1-\boldsymbol{k}_2-\boldsymbol{k}_3)B^*(\boldsymbol{k}_1)B(\boldsymbol{k}_2)B(\boldsymbol{k}_3)\,\mathrm{d}\boldsymbol{k}_1\,\mathrm{d}\boldsymbol{k}_2\,\mathrm{d}\boldsymbol{k}_3 \quad (2.21)$$

where $T(\boldsymbol{k},\boldsymbol{k}_1,\boldsymbol{k}_2,\boldsymbol{k}_3)\,(=T_2)$ is given in Appendix A in terms of $v^{(j)}$, $w^{(2)}$ and $y^{(2)}$. The distinction between the various timescales has been dropped as there is now no ambiguity. This has the same form as the Zakharov equation for water waves, the only difference being the definition of $\omega(\boldsymbol{k})$ and the interaction coefficient $T(\boldsymbol{k},\boldsymbol{k}_1,\boldsymbol{k}_2,\boldsymbol{k}_3)$.

The Zakharov interaction coefficient is of the form

$$T(\boldsymbol{k},\boldsymbol{k}_1,\boldsymbol{k}_2,\boldsymbol{k}_3) = u(\boldsymbol{k},\boldsymbol{k}_1,\boldsymbol{k}_2,\boldsymbol{k}_3)+w^{(2)}(\boldsymbol{k},\boldsymbol{k}_1,\boldsymbol{k}_2,\boldsymbol{k}_3)+\tfrac{1}{4}(1-\alpha^2)\,y^{(2)}(\boldsymbol{k},\boldsymbol{k}_1,\boldsymbol{k}_2,\boldsymbol{k}_3), \quad (2.22)$$

where $u(\boldsymbol{k},\boldsymbol{k}_1,\boldsymbol{k}_2,\boldsymbol{k}_3)$ is composed of terms formed by the product of the second-order interaction coefficients, and where $y^{(2)}(\boldsymbol{k},\boldsymbol{k}_1,\boldsymbol{k}_2,\boldsymbol{k}_3)$ is strictly an interfacial term caused by the nonlinear interactions between the upper and lower fluid. It can easily be shown that the interaction coefficients, which are listed in Appendix A, reduce to those of Stiassnie & Shemer (1984) in the limit that the upper fluid density approaches zero. Also, in the case when both fluids are deep, $d_j\to\infty$, these expressions reduce to the form

$$T(\boldsymbol{k},\boldsymbol{k}_1,\boldsymbol{k}_2,\boldsymbol{k}_3) = \alpha^2\bar{u}(\boldsymbol{k},\boldsymbol{k}_1,\boldsymbol{k}_2,\boldsymbol{k}_3)+w^{(2)}(\boldsymbol{k},\boldsymbol{k}_1,\boldsymbol{k}_2,\boldsymbol{k}_3)+\tfrac{1}{4}(1-\alpha^2)\,y^{(2)}(\boldsymbol{k},\boldsymbol{k}_1,\boldsymbol{k}_2,\boldsymbol{k}_3). \quad (2.23)$$

As the Boussinesq parameter α is increased the term $\bar{u}(\boldsymbol{k},\boldsymbol{k}_1,\boldsymbol{k}_2,\boldsymbol{k}_3)$ becomes more important at the expense of the term $y^{(2)}(\boldsymbol{k},\boldsymbol{k}_1,\boldsymbol{k}_2,\boldsymbol{k}_3)$. For the Boussinesq limit the term $\bar{u}(\boldsymbol{k},\boldsymbol{k}_1,\boldsymbol{k}_2,\boldsymbol{k}_3)$ does not contribute while, as stated before, in the surface wave limit the term $y^{(2)}(\boldsymbol{k},\boldsymbol{k}_1,\boldsymbol{k}_2,\boldsymbol{k}_3)$ has no effect.

3. Derivation of the nonlinear Schrödinger equation

The Zakharov equation can be approximated by a nonlinear Schrödinger equation, coupled with a wave-induced mean-flow equation, under the assumption that the solution is a wavetrain with a long-wavelength modulation. Following Zakharov (1968), Stiassnie & Shemer (1984) we define $\boldsymbol{k}_j=\boldsymbol{k}_0+\boldsymbol{p}_j$, where $\boldsymbol{p}_j=(p_j,q_j)$ and

$$A(\boldsymbol{p},t) = B(\boldsymbol{k},t)\,\mathrm{e}^{-\mathrm{i}(\omega(\boldsymbol{k})-\omega(\boldsymbol{k}_0))t}$$

which, upon substitution into (2.21) gives

$$\mathrm{i}A(\boldsymbol{p})_t-[\omega(\boldsymbol{k})-\omega(\boldsymbol{k}_0)]A(\boldsymbol{p})=\int_{-\infty}^{\infty}\int_{-\infty}^{\infty}\int_{-\infty}^{\infty}T(\boldsymbol{k}_0+\boldsymbol{p},\boldsymbol{k}_0+\boldsymbol{p}_1,\boldsymbol{k}_0+\boldsymbol{p}_2,\boldsymbol{k}_0+\boldsymbol{p}_3)\times A^*(\boldsymbol{p}_1)A(\boldsymbol{p}_2)A(\boldsymbol{p}_3)\,\delta(\boldsymbol{p}+\boldsymbol{p}_1-\boldsymbol{p}_2-\boldsymbol{p}_3)\,\mathrm{d}\boldsymbol{p}_1\,\mathrm{d}\boldsymbol{p}_2\,\mathrm{d}\boldsymbol{p}_3. \quad (3.1)$$

The simplification which leads to the nonlinear Schrödinger equation is the assumption that the solution to the Zakharov equation is a wavetrain with a slow spatial variation. This implies that the Fourier transform of this wavetrain is band limited and that this band width is assumed to behave as the wave steepness. That is, $\boldsymbol{p}_j/k_0=O(k_0 a)$. Under this assumption

$$\omega(\boldsymbol{k})-\omega(\boldsymbol{k}_0)=\boldsymbol{c}_g\cdot\boldsymbol{p}+\frac{c_g}{2k_0}q^2+\tfrac{1}{2}c_g' p^2+O((k_0a)^3),$$

where $\boldsymbol{c}_g$ is the group velocity of the carrier wave and c_g' is the modulus of its derivative with respect to k. From (2.16) it can be shown that the surface height is given by the expression

$$\eta(\boldsymbol{x})=\frac{1}{2\pi}\left(\frac{|\boldsymbol{k}_0|\lambda(\boldsymbol{k}_0)}{2\omega(\boldsymbol{k}_0)}\right)^{\frac{1}{2}}\mathrm{e}^{\mathrm{i}(\boldsymbol{k}_0\cdot\boldsymbol{x}-\omega(\boldsymbol{k}_0)t)}\int_{-\infty}^{\infty}A(\boldsymbol{p})\,\mathrm{e}^{\mathrm{i}\boldsymbol{p}\boldsymbol{x}}\,\mathrm{d}\boldsymbol{p}+\text{c.c.},$$

to leading order in spectral width. The complex wave amplitude is then

$$a(\boldsymbol{x},t)\approx\left(\frac{2k_0\lambda(\boldsymbol{k}_0)}{\omega(\boldsymbol{k}_0)}\right)^{\frac{1}{2}}F^{-1}\{A(\boldsymbol{p})\}, \quad (3.2)$$

where $F^{-1}\{\,\}$ defines the inverse Fourier transform operation. Taking the inverse Fourier transform of (3.1) one obtains

$$\mathrm{i}(a_t+c_g a_x)+\tfrac{1}{2}c_g' a_{xx}+\frac{c_g}{2k_0}a_{yy}=\frac{1}{2\pi}\left(\frac{2k_0\lambda(\boldsymbol{k}_0)}{\omega(\boldsymbol{k}_0)}\right)^{\frac{1}{2}}\times\int_{-\infty}^{\infty}\int_{-\infty}^{\infty}\int_{-\infty}^{\infty}\int_{-\infty}^{\infty}T(\boldsymbol{k}_0+\boldsymbol{p},\boldsymbol{k}_0+\boldsymbol{p}_1,\boldsymbol{k}_0+\boldsymbol{p}_2,\boldsymbol{k}_0+\boldsymbol{p}_3)\times A^*(\boldsymbol{k}_1)A(\boldsymbol{k}_2)A(\boldsymbol{k}_3)\,\mathrm{e}^{\mathrm{i}(\boldsymbol{p}_2+\boldsymbol{p}_3-\boldsymbol{p}_1)\cdot\boldsymbol{x}}\,\delta(\boldsymbol{p}+\boldsymbol{p}_1-\boldsymbol{p}_2-\boldsymbol{p}_3)\,\mathrm{d}\boldsymbol{p}\,\mathrm{d}\boldsymbol{p}_1\,\mathrm{d}\boldsymbol{p}_2\,\mathrm{d}\boldsymbol{p}_3. \quad (3.3)$$

As this is to be truncated to third order, then only the component of $A(\boldsymbol{p}_j)$ evaluated at $\boldsymbol{p}_j=0$ is to be kept and hence only the leading term of the Zakharov interaction coefficient is necessary, viz.

$$T(\boldsymbol{k}_0+\boldsymbol{p},\boldsymbol{k}_0+\boldsymbol{p}_1,\boldsymbol{k}_0+\boldsymbol{p}_2,\boldsymbol{k}_0+\boldsymbol{p}_3)\approx\mu_0(\boldsymbol{k}_0)+\mu_1(\boldsymbol{k}_0,\boldsymbol{p}_3-\boldsymbol{p}_1)+O(\boldsymbol{p}_j/k_0),$$

where $\mu_1\rightarrow 0$ as $q_3-q_1\rightarrow 0$. The dependence of μ_1 on $\boldsymbol{p}_3$ and $\boldsymbol{p}_1$ is in terms of the expression $\boldsymbol{k}_0\cdot(\boldsymbol{p}_3-\boldsymbol{p}_1)/k_0|\boldsymbol{p}_3-\boldsymbol{p}_1|$ alone. That is, the value of μ_1 is dependent on the angle between the difference of the perturbation wavenumbers, and the wavenumber of the main wave. This gives

$$\mathrm{i}(a_t+c_g a_x)+\tfrac{1}{2}c_g' a_{xx}+\frac{c_g}{2k_0}a_{yy}=2\pi^2\frac{\omega(\boldsymbol{k}_0)}{|\boldsymbol{k}_0|\lambda(\boldsymbol{k}_0)}(a|a|^2\mu_0(\boldsymbol{k}_0)+aQ) \quad (3.4a)$$

where

$$Q=\frac{1}{4\pi^2}\int_{-\infty}^{\infty}\mu_1(\boldsymbol{k}_0,\boldsymbol{p})\,\mathrm{e}^{-\mathrm{i}\boldsymbol{p}\cdot\boldsymbol{x}}\left[\int_{-\infty}^{\infty}|a|^2\,\mathrm{e}^{\mathrm{i}\boldsymbol{p}\cdot\boldsymbol{x}}\,\mathrm{d}\boldsymbol{x}\right]\mathrm{d}\boldsymbol{p}$$

$$=F^{-1}\{\mu_1(\boldsymbol{k}_0,\boldsymbol{p})\,F\{|a|^2\}\}.$$

The above integral expression is equivalent to the differential equation

$$\mathrm{L}Q = \mathrm{M}\frac{\partial^2}{\partial y^2}|a|^2, \tag{3.4b}$$

where

$$\mathrm{L} = (c_g^2 k_0^2 - w_p^2)\,(c_g^2 k_0^2 \frac{\partial^2}{\partial x^2} - w_p^2 \nabla_x^2)\,\nabla_x^2,$$

$$\mathrm{M} = k_0^2 \omega^2(\boldsymbol{k}_0)\,(\chi_1 \omega_p^2 + c_g^2 k_0^2 \chi_2)\,\nabla_x^2 - \chi_3 k_0^3 (k_0^2 c_g^2 - w_p^2)\,(c_g^2 k_0^2 \frac{\partial^2}{\partial x^2} - \omega_p^2 \nabla_x^2),$$

and χ_1, χ_2, χ_3 and ω_p are defined in Appendix B.

The equations (3.4) were first derived by Grimshaw & Pullin (1985) where it was shown that Q represented the part of the wave-induced mean flow that responds to transverse modulations. These also reduce to the Davey–Stewartson equations when the upper density is zero. With the substitution of

$$\xi = \epsilon(\boldsymbol{x} - c_g t) \quad \text{and} \quad \tau = \epsilon^2 t,$$

that is, in a frame moving with the group velocity, one obtains

$$\mathrm{i}a_\tau + \tfrac{1}{2}c_g' a_{\xi\xi} + \frac{c_g}{2k_0} a_{yy} = 2\pi^2 a \frac{\omega(\boldsymbol{k}_0)}{\boldsymbol{k}_0 \lambda(\boldsymbol{k}_0)} (\mu_0(\boldsymbol{k}_0)|a|^2 + Q).$$

If it is assumed that both a and Q have solutions with spatial dependence in terms of $\xi_1 = p\xi + qy$, that is are modulated in a single direction specified by the direction of the wavenumber $\boldsymbol{p}$, then (3.4) reduce to

$$\mathrm{i}a_\tau + \left(\tfrac{1}{2}c_g' p^2 + \frac{c_g}{2k_0} q^2\right) a_{\xi_1 \xi_1} = 2\pi^2 a|a|^2 \frac{\omega(\boldsymbol{k}_0)}{\boldsymbol{k}_0 \lambda(\boldsymbol{k}_0)} (\mu_0(\boldsymbol{k}_0) + \mu_1(\boldsymbol{k}_0, \boldsymbol{p})). \tag{3.5}$$

The coefficients $\mu_0(\boldsymbol{k}_0)$ and $\mu_1(\boldsymbol{k}_0, \boldsymbol{p})$ are given in Appendix B and are in agreement with the cubic term of the nonlinear Schrödinger equation that was derived by Grimshaw & Pullin (1985) after the change of scale such that $\eta_1 = 2\pi k_0 a$ is made. The term η_1 is the dependent variable used in this paper.

4. Linear stability analysis

4.1. *Calculation of the basic state*

A relatively simple solution to the Zakharov equation can be found by looking for a uniform, two-dimensional travelling wave. Set

$$B(\boldsymbol{k}, t) = \hat{B}_s(t)\,\delta(\boldsymbol{k} - \boldsymbol{k}_0). \tag{4.1}$$

Substitution into (2.21) then gives

$$\mathrm{i}\hat{B}_{s,t}(t)\,\delta(\boldsymbol{k} - \boldsymbol{k}_0) = T(\boldsymbol{k}, \boldsymbol{k}_0, \boldsymbol{k}_0, \boldsymbol{k}_0)\,|\hat{B}_s(t)|^2 \hat{B}_s(t)\,\delta(\boldsymbol{k} - \boldsymbol{k}_0).$$

This has a solution for $\hat{B}_s(t)$ of the form

$$\hat{B}_s(t) = B_0 \lim_{\boldsymbol{k} \to \boldsymbol{k}_0} \mathrm{e}^{-\mathrm{i}B_0^2 T(\boldsymbol{k}, \boldsymbol{k}_0, \boldsymbol{k}_0, \boldsymbol{k}_0)t} = B_0\,\mathrm{e}^{-\mathrm{i}B_0^2 \mu(\boldsymbol{k}_0)t}, \tag{4.2}$$

for a strictly two-dimensional wave. To leading order it can be shown that

$$\eta(\boldsymbol{x}, t) = \frac{B_0}{\pi}\left(\frac{|\boldsymbol{k}_0|\lambda(\boldsymbol{k}_0)}{2\omega(\boldsymbol{k}_0)}\right)^{\frac{1}{2}} \cos\left(\boldsymbol{k}_0 \cdot \boldsymbol{x} - (\omega(\boldsymbol{k}_0) + B_0^2 \mu_0(\boldsymbol{k}_0))\,t\right),$$

with the use of (2.16). This is a periodic wave with the nonlinear correction to the phase velocity $B_0^2 \mu_0(\boldsymbol{k}_0)$. This nonlinear correction, which is identical to that found by Grimshaw & Pullin (1985, equation (4.5)), takes the form of the standard Stokes correction together with a wave-induced 'drift speed', i.e. a mean-flow term. This also reduces to that given by Davey & Stewartson (1974) for the surface wave case.

4.2. *Linear stability analysis of a perturbation to the basic state*

In the usual manner the stability of this solution is examined by adding a small perturbation, viz.

$$B(\boldsymbol{k},t) = \hat{B}_s(t)\,\delta(\boldsymbol{k}-\boldsymbol{k}_0) + \hat{B}_+(t)\,\delta(\boldsymbol{k}+\boldsymbol{p}-\boldsymbol{k}_0) + \hat{B}_-(t)\,\delta(\boldsymbol{k}-\boldsymbol{p}-\boldsymbol{k}_0), \tag{4.3}$$

where it is assumed that $\hat{B}_\pm \ll \hat{B}_s$. This perturbation is of the form of a pair of plane waves with wavenumbers $\boldsymbol{k}_0 \pm \boldsymbol{p}$. By substituting this into (2.21), and linearizing in $\hat{B}_\pm$, it was shown by Crawford *et al.* (1981) that the coupled equation

$$\mathrm{i}\frac{\mathrm{d}\hat{B}_\pm}{\mathrm{d}t} = T_{\pm\mp} B_0^2 \hat{B}_\mp^* \,\mathrm{e}^{-\mathrm{i}(\Omega + 2T_0 B_0^2)t} + 2T_{\pm,\pm} B_0^2 \hat{B}_\pm \tag{4.4}$$

is obtained, where

$$\left.\begin{aligned} T_{\pm,\pm} &= \tfrac{1}{2}(T(\boldsymbol{k}_0\pm\boldsymbol{p},\boldsymbol{k}_0,\boldsymbol{k}_0,\boldsymbol{k}_0\pm\boldsymbol{p}) + T(\boldsymbol{k}_0\pm\boldsymbol{p},\boldsymbol{k}_0,\boldsymbol{k}_0\pm\boldsymbol{p},\boldsymbol{k}_0)),\\ T_{\pm\mp} &= T(\boldsymbol{k}_0\pm\boldsymbol{p},\boldsymbol{k}_0\mp\boldsymbol{p},\boldsymbol{k}_0,\boldsymbol{k}_0)\end{aligned}\right\} \tag{4.5}$$

and

$$\Omega = 2\omega(\boldsymbol{k}_0) - \omega(\boldsymbol{k}_0+\boldsymbol{p}) - \omega(\boldsymbol{k}_0-\boldsymbol{p}).$$

This can be solved with the substitution of the relation

$$\hat{B}_\pm(t) = B_\mp\,\mathrm{e}^{-\mathrm{i}(\frac{1}{2}\Omega + \mu_0 B_0^2 \pm s)t}, \tag{4.6}$$

where $B_\pm$ and s are constants. This gives s to be

$$s = (T_{+,+} - T_{-,-})B_0^2 \pm \{-T_{+,-}T_{-,+}B_0^4 + [-\tfrac{1}{2}\Omega + B_0^2(T_{+,+} + T_{-,-} - \mu_0)]^2\}^{\frac{1}{2}}. \tag{4.7}$$

By (4.6) the only possible situation where there could be a growth in the perturbation is when s becomes complex. For small wave steepnesses, this implies that the value of Ω is small and hence instabilities are due to resonant quartets at or near the curve in $\boldsymbol{p}$-space defined by $\Omega = 0$, recovering (1.1). This does not preclude the possibility of other forms of instabilities for finite wave steepnesses.

The valuation of (4.7) was not straightforward, because the term

$$T(\boldsymbol{k},\boldsymbol{k}_1,\boldsymbol{k}_2,\boldsymbol{k}_3) = T(\boldsymbol{k}_0\pm\boldsymbol{p},\boldsymbol{k}_0,\boldsymbol{k}_0\pm\boldsymbol{p},\boldsymbol{k}_0)$$

is singular for all values of $\boldsymbol{p}$. This singularity was found to be removable as both numerator and denominator are of the same order in the limit that $\boldsymbol{k}_2 \to \boldsymbol{k}$. The local solution was found for these singular terms, that is, the limit

$$\lim_{\delta\to 0} T(\boldsymbol{k}_0\pm\boldsymbol{p}+\delta,\boldsymbol{k}_0,\boldsymbol{k}_0\pm\boldsymbol{p},\boldsymbol{k}_0)$$

was found in terms of $\boldsymbol{k}_0$, $\boldsymbol{p}$ and, unfortunately, the direction of the vector $\boldsymbol{\delta}$. Although individually they were found to be dependent upon the direction as $\boldsymbol{\delta}$ approached zero, it was found that

$$T_{+,+} + T_{-,-} - (\mu_0 + \mu_1(\boldsymbol{\delta}))$$

was directionally independent, where the wavenumber of the main wave was also perturbed by $\boldsymbol{\delta}$. That is, as long as the direction of $\boldsymbol{\delta}$ was kept the same for the

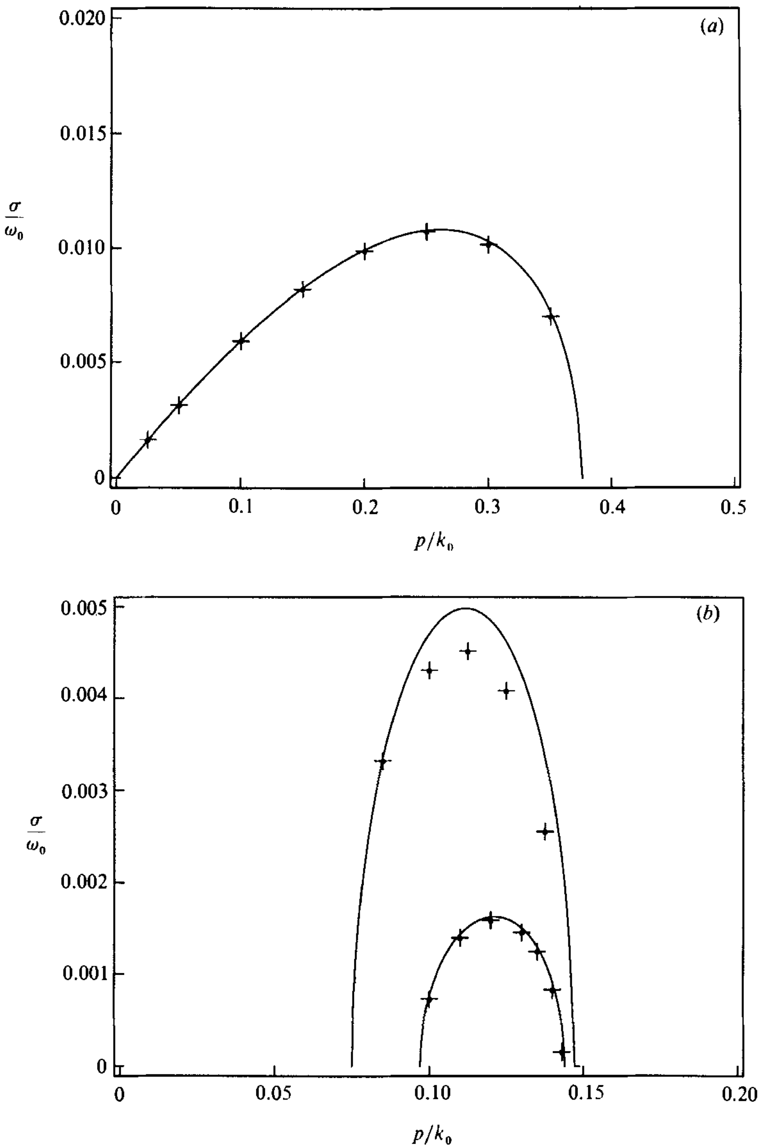

FIGURE 2. Comparison of present results (continuous line) with the numerical results of Pullin & Grimshaw (1985) (+): $\sigma/\omega(k_0)$ *vs.* p/k_0. (*a*) $k_0 a = 0.1\pi$, $k_0 d_1 = 10\pi$, $k_0 d_2 = \infty$, $q/k_0 = 0$; (*b*) $k_0 a = 0.02\pi$, 0.05π (lower), $k_0 d_1 = 0.2\pi$, $q/k_0 = 0.1$.

evaluation of all the terms then the growth rate did not depend on this direction. Physically, this $\boldsymbol{\delta}$ has the effect of a long-wavelength modulation to the system which would be the same for all the interaction coefficients. The value of s could then be evaluated for a given $\boldsymbol{p}$. This complication does not arise for the infinite-depth case as these singular terms decay algebraically with depth.

As it is known that the regions of instability will be restricted to the region near the 'figure of 8' curve, at least for small wave steepnesses, then for a given q there will be four distinct zeros to the expression within the square root of (4.7), for p and q positive. These roots were found using the secant method. The two intervals of instability were subdivided, generally into twenty equispaced divisions, so that the growth rates could be found for the various values of p within this region. This was repeated for a range of q that encompassed the 'figure of 8' curve.

These results were compared with those of Pullin & Grimshaw (1985) for the Boussinesq limit and Stiassnie & Shemer (1984) for the surface wave case. The results were identical to the latter, as would be expected, thus checking the computer code. The difference between the author's results and the numerical results of Pullin & Grimshaw (1985) were surprisingly small for all reasonable values of wave steepness. This can be seen in figure 2. It should be pointed out that for the case of surface waves the agreement is not as good between the Zakharov equation and the numerical results for the same wave steepness, see Stiassnie & Shemer (1984).

5. Results

For small wave steepnesses the quartet instabilities are restricted to the 'figure of 8' curve given by (1.1). Only the growth rates for p, q positive were investigated owing to the inherent symmetries, i.e. the growth rates were invariant under reflection about $p = 0$ or $q = 0$. These growth rates σ, the imaginary part of s, were divided by the square of the wave steepness, a normalization suggested by (4.7). The perturbation wavenumbers were normalized with respect to the wavenumber of the main wave. For convenience the region on this curve where q is increasing with increasing p is termed the region of small p while the region of decreasing q with increasing p is termed the region of large p. Three values of the Boussinesq parameter were investigated: 0, 0.8 and 1.

The growth rates for various values of the two depths, d_1, d_2 are shown in figures 3–6. For both depths infinite, figure 3, the perturbation wavenumber of the largest growth rate is always small and in the direction of the main wave, this point is represented by a dot in the figures. For the surface wave case, $\alpha = 1$, the region of large p is stable, in agreement with previous surface wave results, but becomes unstable as the Boussinesq parameter is decreased. It was found numerically that the width of the region of instability near $\boldsymbol{p} \approx (1.25, 0)$ behaves as

$$(k_0 a)^2 (1-\alpha^2),$$

implying that the surface wave case is exceptional in that the region of large p does not exhibit instability at order $(k_0 a)^2$. McLean (1982*a*) showed that this region actually possesses growth rates of order $(k_0 a)^4$ and so would not appear at this lower order.

As the lower depth was decreased it was found that the growth rates for small perturbation wavenumbers decreased with eventual restabilization for all values of the Boussinesq parameter, in agreement with Grimshaw & Pullin (1985), Whitham (1967) etc., with the Boussinesq limit being more sensitive. This caused the perturbation wavenumber of greatest growth rate to generally become three-dimensional, i.e. oblique to the main wave. For the surface wave case the region of large p is now unstable and for very small lower layer depths, $k_0 d_2 \approx 0.2\pi$, it was found that the perturbation wavenumber of greatest growth rates was in fact two-dimensional but in the region of large p, in agreement with McLean (1982*b*). The effect of decreasing the upper depth with $\alpha = 0.8$ was to again decrease the growth rates for small perturbation wavenumbers, but not nearly to the same extent as when the lower depth was decreased. For the Boussinesq limit, decreasing the lower depth initially increased the growth rates for the region of large p, to the point that the wavenumber of greatest growth rate became two-dimensional and in this region, e.g.

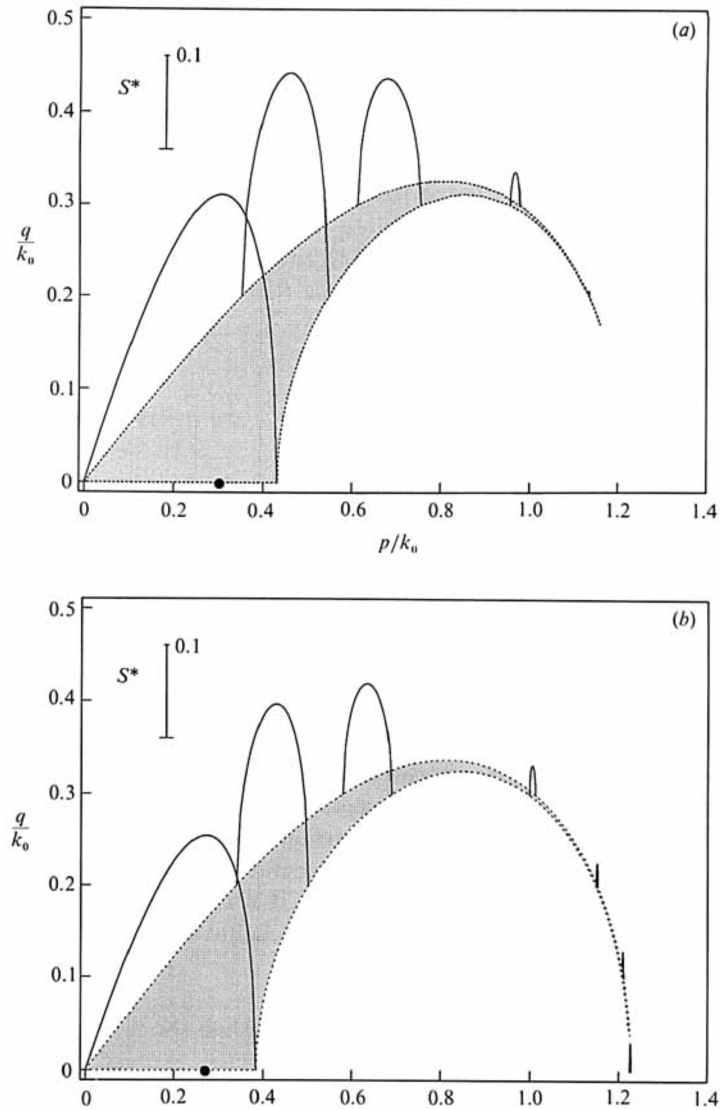

FIGURE 3(a,b). For caption see facing page.

figure 4(c). As the depth was further reduced, however, the growth rate in this region decreased so that the wavenumber of greatest instability was again three-dimensional and in the region of small p. It can be shown, see Appendix A, that in the Boussinesq limit if the values of the two depths are interchanged the growth rates remain the same. Hence decreasing the upper depth will produce the same results as decreasing the lower depth.

In figure 5 the effect of decreasing both depths is shown. This is a region that the previous numerical studies for interfacial waves did not investigate. For $\alpha = 0.8$ it is very similar to when the lower depth was decreased alone. For $\alpha = 0$ the whole region of small p has nearly restabilized as predicted by the nonlinear Schrödinger equation, Grimshaw & Pullin (1985). The perturbation wavenumber of greatest growth rates is now two-dimensional in the region of large p.

It was found that increasing the wave steepness increased the resonant bandwidth

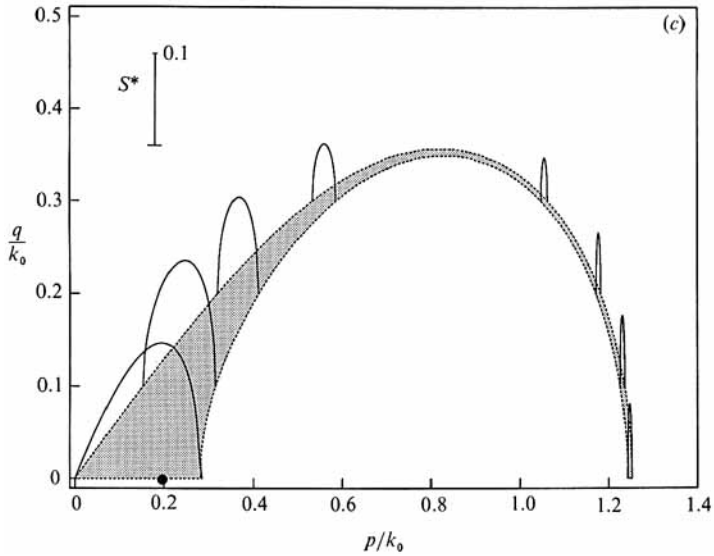

FIGURE 3. Stability diagrams with superimposed growth rates (at q/k_0 = constant) – shaded regions are unstable, $s^* = \sigma\lambda(\boldsymbol{k}_0)/\omega(\boldsymbol{k}_0)\,(k_0 a)^2$; ●, position of largest growth rate. $k_0 a = 0.2$, $k_0 d_1 = k_0 d_2 = \infty$. (*a*) $\alpha = 1.0$, (*b*) $\alpha = 0.8$, (*c*) $\alpha = 0$.

but decreased the dimensions of the 'figure of 8' as was previously found for surface waves e.g. Crawford *et al.* (1981). For the infinite-depth surface wave case it was found that for wave steepnesses greater than 0.39 the resonant band left the point $\boldsymbol{p} = (0,0)$ and by about 0.5 there is complete restabilization, again in agreement with Crawford *et al.* (1981). Decreasing the depth in this wave steepness region had a destabilizing effect. The trend is similar for $\alpha = 0.8$ with restabilization of the region of small p at $k_0 a = 0.58$ for both depths infinite. Again, decreasing the lower depth produced a destabilizing effect while the effect of decreasing the upper depth was negligible. The region of large p did not restabilize for reasonable values of $k_0 a$, however. For $\alpha = 0$, the region of small p never completely restabilized but the growth rates reached a minimum at $k_0 a \approx 0.79$. Again, the region of large p did not restabilize. This is shown in figure 6. The numerical method of Pullin & Grimshaw (1985) could not investigate this region of wave steepness and Boussinesq parameter as it was swamped by the Kelvin–Helmholtz instability.

It appears that restabilization of quartet resonances is restricted to the infinite-depth surface wave case owing to the general instability at large p at other values of the Boussinesq parameter. This region of Boussinesq parameter was investigated to see if restabilization occurred for the case of air over water. This is shown in figure 7 where the wave steepness of restabilization for the region $\boldsymbol{p} \approx (1.25, 0)$ is plotted against the Boussinesq parameter, the region of small p being insensitive to these changes. It was found that restablization is possible for $\alpha > 0.97$ for reasonable wave steepnesses, which includes the case of air over water, $\alpha \approx 0.9967$.

As the derivation of the Zakharov equation is based on a small-amplitude approximation, these last sets of results must be viewed with caution. It is encouraging to note that although, for the case of surface waves, restabilization took place at a value of the wave steepness far in excess of what would normally be considered valid it does predict the qualitative results. This wave steepness of restabilization is actually higher than the wave of greatest steepness, while for the

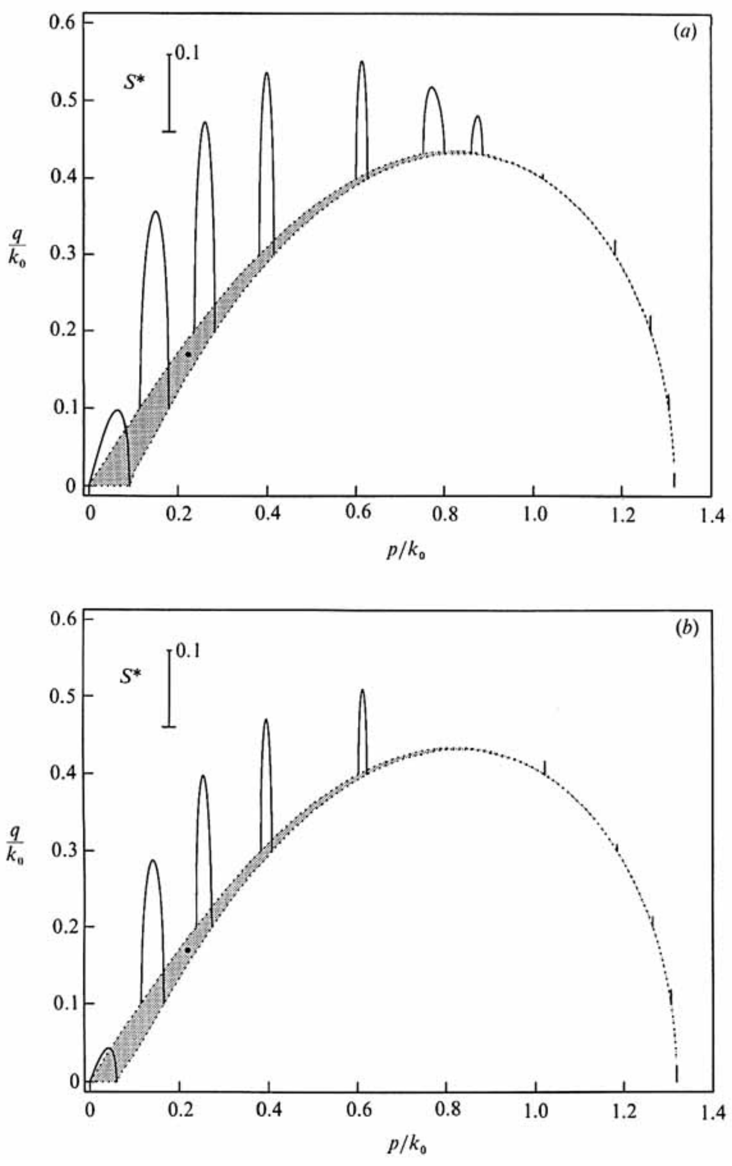

FIGURE 4 (a, b). For caption see facing page.

Boussinesq limit the wave steepness of near restabilization is approximately 60 % of that of the highest wave.

6. Investigation of a wave-induced Kelvin–Helmholtz instability

Another form of instability was found for the case of large perturbation wavenumbers. This was confined to when the Boussinesq parameter is small and for a moderately large wave steepness. This is due to a Kelvin–Helmholtz instability and is caused by the jump in fluid velocity across the interface due to the main wave. This is probably related to a similar instability found by Pullin & Grimshaw (1985), who first suggested this interpretation.

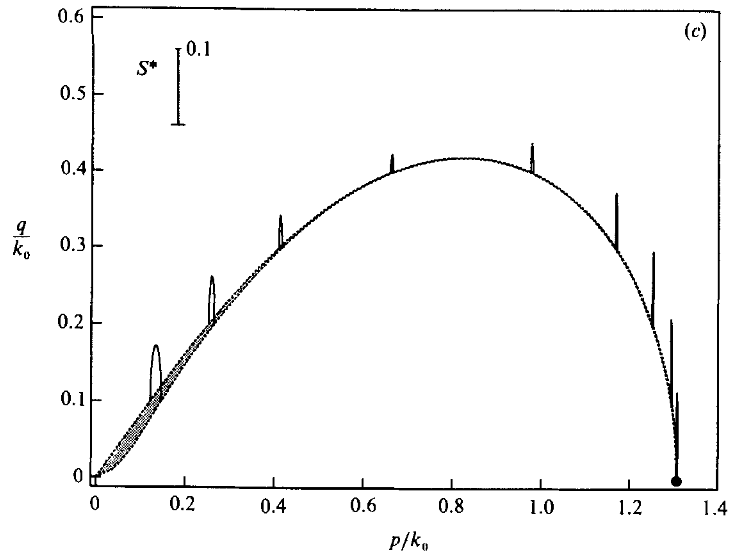

FIGURE 4. Stability diagram with superposed growth rates, $s^* = \sigma\lambda(k_0)/\omega(k_0)\,(k_0 a)^2$. $k_0 a = 0.1$, $k_0 d_1 = 3\pi$, $k_0 d_2 = \frac{1}{2}\pi$. (*a*) $\alpha = 1.0$, (*b*) $\alpha = 0.8$, (*c*) $\alpha = 0$.

This instability was found to take the form of a band in the (p, q)-plane, as can be seen in figure 8. Note that these growth rates are much larger than for the quartet resonance. As the wave steepness was increased the band became smaller in width and approached the origin. The growth rates also decreased in magnitude. Increasing the Boussinesq parameter was found to have a stabilizing effect. The numerical results did not give this banded structure and it is shown in Appendix C to be not real but due to the limitations of the Zakharov equation for large perturbation wavenumbers.

The above mentioned Kelvin–Helmholtz instability can be investigated with the use of a simple analytic model. As large wavenumber perturbations are being investigated on a basic wave of small steepness, the latter can be approximated by an interface that is locally flat and horizontal, and with a velocity field that is constant compared to the lengthscales of the perturbations. The dispersion relation for such a system in the Boussinesq limit is given by

$$s^{\pm}(\boldsymbol{p}) = -\tfrac{1}{2}p(U_1+U_2) \pm \mathrm{i}(\tfrac{1}{4}p^2(U_2-U_1)^2 - g\alpha|\boldsymbol{p}|)^{\frac{1}{2}}, \quad (6.1)$$

where U_2 and U_1 are the mean fluid velocities on either side of the interface and $\boldsymbol{p}$ is the wavenumber of the perturbation, see Drazin & Reid (1981). To obtain an approximation to U_j the linearized equations of (2.1) and (2.2) can be used to obtain

$$\eta(\boldsymbol{x}, t) = a\cos(\boldsymbol{k}_0\cdot\boldsymbol{x} - \omega(\boldsymbol{k}_0)\,t) + O((k_0 a)^2),$$

$$\phi_j(\boldsymbol{x}, z, t) = \frac{(-1)^j}{k_0} a\omega(\boldsymbol{k}_0)\sin(\boldsymbol{k}_0\cdot\boldsymbol{x} - \omega(\boldsymbol{k}_0)\,t)\,\mathrm{e}^{(-1)^j|\boldsymbol{k}_0|z} + O((k_0 a)^2)$$

for the main wave. As $U_j = \phi_{j,x}\,(\boldsymbol{x}, 0, t)$ then from (6.1) the growth rates are found to be

$$\sigma(\boldsymbol{p})/\omega(\boldsymbol{k}_0) = (p^2\eta^2(\boldsymbol{x}, t) - |\boldsymbol{p}|/k_0)^{\frac{1}{2}} + O((k_0 a)^2) \quad (6.2)$$

for $$|\boldsymbol{p}|/k_0 > 1/k_0^2\eta^2\cos^2\phi = p_c/k_0\cos^2\phi,$$

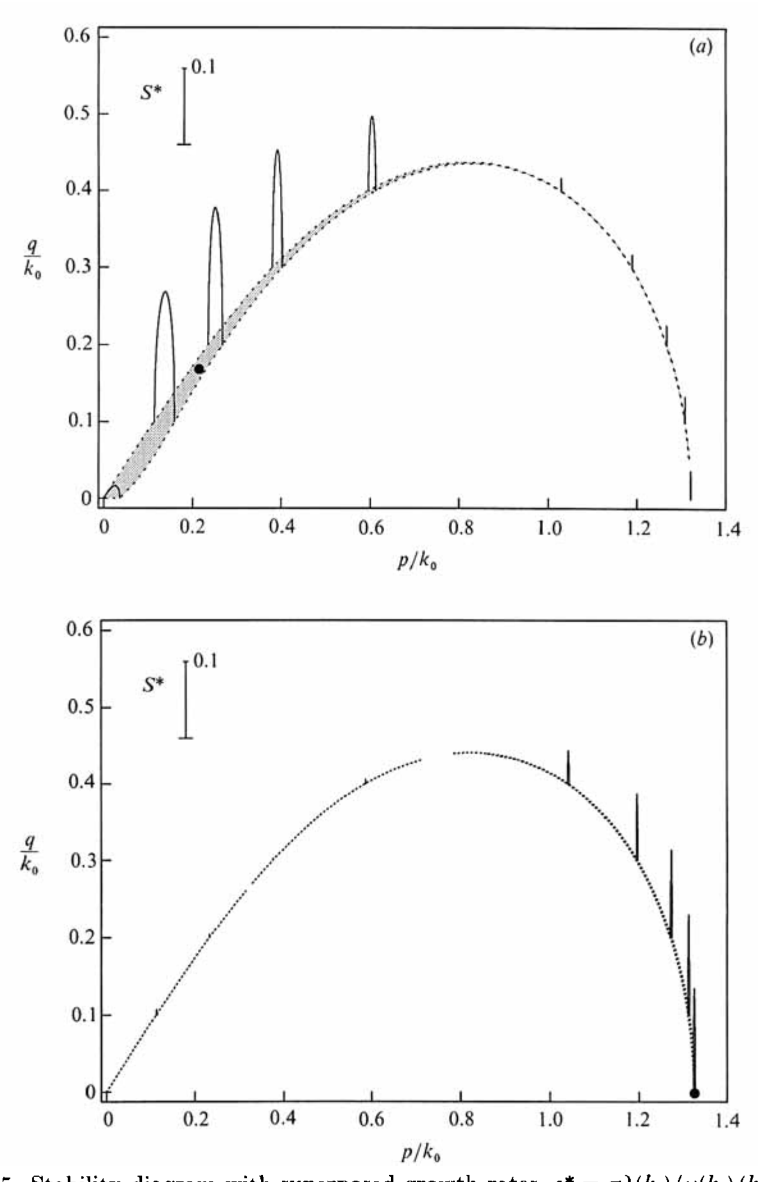

FIGURE 5. Stability diagram with superposed growth rates, $s^* = \sigma\lambda(k_0)/\omega(k_0)\,(k_0 a)^2$. $k_0 a = 0.1$, $k_0 d_1 = k_0 d_2 = \frac{1}{2}\pi$. (a) $\alpha = 0.8$, (b) $\alpha = 0$.

where ϕ is the angle between the perturbation and the main wave. Instability is therefore greatest at the crests and troughs.

These expressions agree well with the numerical results of Pullin & Grimshaw (1985) but not with the present results as there is no restabilization for large $|\boldsymbol{p}|$. The banded structure is due to the exclusion of the rapidly varying terms of (2.20) to obtain the Zakharov equation, hence only part of the instability is described. This is discussed further in Appendix C where these non-resonant terms are included and (6.2) is rederived from (2.18).

It should be noted that these growth rates are of order $p\eta \gg 1$ for $|\boldsymbol{p}| \gg p_c$ in conflict with (2.19) where it was assumed that the system evolves at a rate $(k_0 a)^2$. In

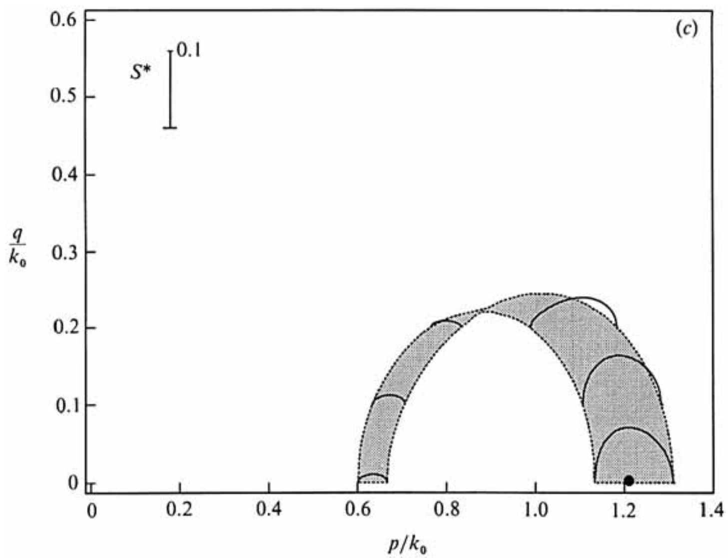

FIGURE 6. Partial restabilization at large wave steepnesses, $s^* = \sigma\lambda(k_0)/\omega(k_0)\,(k_0 a)^2$. $k_0 a = 0.85$, $k_0 d_1 = k_0 d_2 = \infty$, $\alpha = 0$.

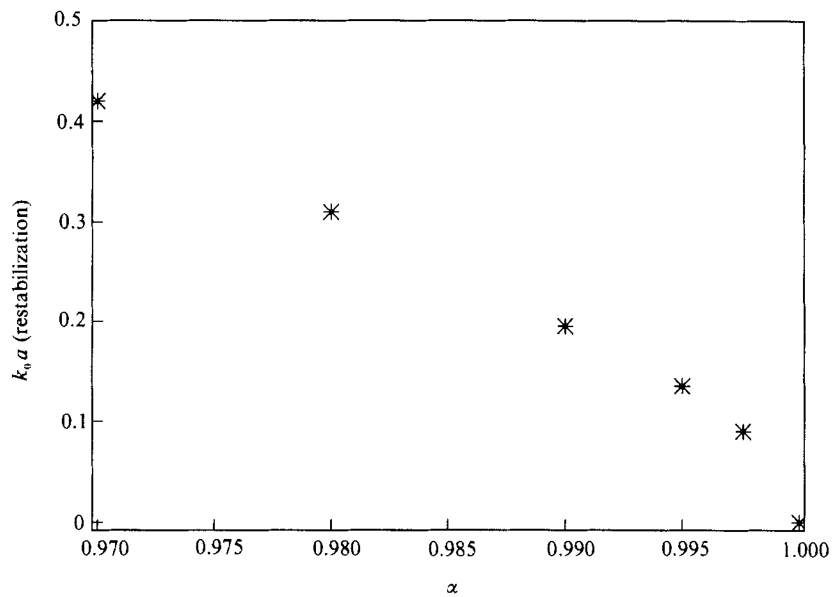

FIGURE 7. Wave steepness of restabilization for large p for various values of the Boussinesq parameter: $k_0 a$ *vs.* α. $k_0 d_1 = k_0 d_2 = \infty$, $p \approx 1.25$, $q = 0$.

reality one would expect the growth rates to be limited at these high wavenumbers by the effects of surface tension, viscosity and/or the finite thickness of the interface.

For example if surface tension were to be included then (6.2) would become

$$\sigma(\boldsymbol{p})/\omega(\boldsymbol{k}_0) = \left(p^2\eta^2(\boldsymbol{x},t) - |\boldsymbol{p}|/k_0 - \frac{\gamma}{\rho\omega^2(\boldsymbol{k}_0)}|\boldsymbol{p}|^3\right)^{\frac{1}{2}} + O((k_0 a)^2), \tag{6.3}$$

where γ is the coefficient for the interfacial surface tension. Note that for a given $|\boldsymbol{p}|$

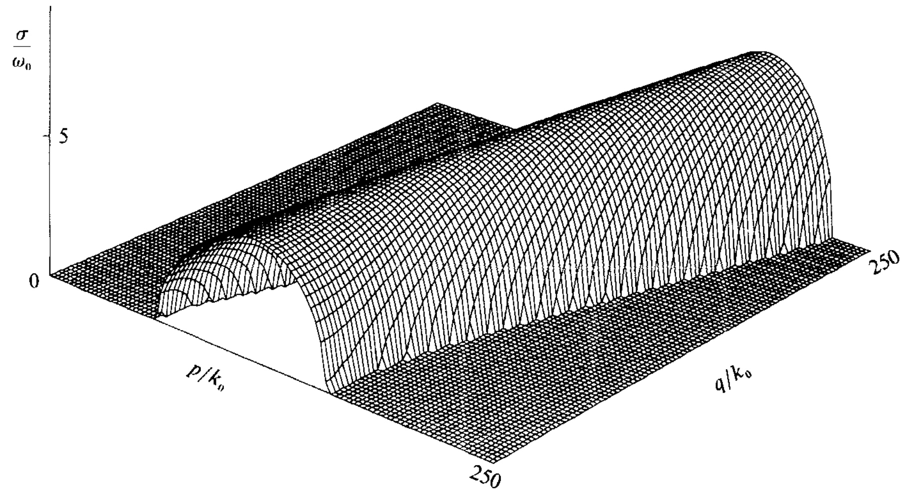

FIGURE 8. Large wavenumber Kelvin–Helmholtz instability: $\sigma/\omega(k_0)$ *vs.* $(p/k_0, q/k_0)$. $k_0 a = 0.2$, $k_0 d_1 = k_0 d_2 = \infty$, $\alpha = 0$.

instability is greatest for perturbations parallel to the main wave. Instability is now restricted to the wavenumber band

$$\tfrac{1}{2}\Gamma^{-1}[1-(1-4\Gamma/(k_0\eta\cos\phi)^4)^{\frac{1}{2}}] < \frac{|p|/k_0}{(k_0\eta\cos\phi)^2} < \tfrac{1}{2}\Gamma^{-1}[1+(1-4\Gamma/(k_0\eta\cos\phi)^4)^{\frac{1}{2}}],$$

where
$$\Gamma = \gamma k_0^3/\rho\omega^2(\boldsymbol{k}_0),$$

so that high wavenumbers have restabilized with the addition of surface tension. This implies that for a region to be unstable then

$$|\eta(\boldsymbol{x},t)| > (4\Gamma)^{\frac{1}{4}}/k_0,$$

that is, the Kelvin–Helmholtz instability is restricted to regions of the main wave where the interface is of a vertical distance greater than $(4\Gamma)^{\frac{1}{4}}/k_0$ above or below the mean level. As an example consider the case of ether, with a density of 0.736 g/cc, on water. The Boussinesq parameter is 0.152 and for a wavelength of the main wave of 20 cm then $\Gamma = 0.0041$, giving $|\eta| > 1.1$ cm for instability.

7. Conclusion

Two forms of instabilities were found for interfacial waves from the Zakharov equation. The first is due to a quartet interaction, similar to that for the surface wave case, while the second is a Kelvin–Helmholtz instability and appears for large perturbation wavenumbers and small values of the Boussinesq parameter. This latter form of instability has large growth rates and is restricted to a band in the (p,q)-plane. This band structure, however, is due to the limitations of the Zakharov equation for large perturbation wavenumbers and is not real.

For the resonant quartet instability, the dependence of growth rates on the Boussinesq parameter and the two depths was found to be complex. The general trend, however, was that as one of the depths was decreased the growth rate near the origin reduced and eventually restabilized. This caused the wavenumber of greatest instability to become three-dimensional except in certain cases when the dominant instability was then in the region of large p with $q = 0$. This was found for both small-depth surface waves and for a limited range of depths in the Boussinesq limit.

The restabilization of quartet resonances at large values of the wave steepness was restricted to the case of infinite-depth surface waves, as it was only for this case that the region of large p on the 'figure of 8' was stable. Higher-order resonances, not incuded in this perturbation approach, remain unstable at these wave steepnesses, however. For decreased values of the Boussinesq parameter this region destabilized but not sufficiently quickly for the case of air on water to be excluded from large wave steepness restabilization. Here again this region of large p was the region of greatest instability for quartet resonance for these wave steepnesses, for all values of the Boussinesq parameter small enough for the waves to be unstable.

I would like to thank Professor R. Grimshaw for his advice and general support with this research. I also wish to thank Professor E. O. Tuck and gratefully acknowledge the support by the Australian Research Council for part of this research.

Appendix A

A.1. *Interaction coefficients for the Zakharov equation*

The interaction coefficient of the Zakharov equation is given by

$$T(\boldsymbol{k},\boldsymbol{k}_1,\boldsymbol{k}_2,\boldsymbol{k}_3) = u(\boldsymbol{k},\boldsymbol{k}_1,\boldsymbol{k}_2,\boldsymbol{k}_3)+w^{(2)}(\boldsymbol{k},\boldsymbol{k}_1,\boldsymbol{k}_2,\boldsymbol{k}_3)+\tfrac{1}{4}(1-\alpha^2)\,y^{(2)}(\boldsymbol{k},\boldsymbol{k}_1,\boldsymbol{k}_2,\boldsymbol{k}_3),$$

where

$$u(\boldsymbol{k},\boldsymbol{k}_1,\boldsymbol{k}_2,\boldsymbol{k}_3) =$$

$$-\frac{v^{(1)}(\boldsymbol{k},\boldsymbol{k}_2,\boldsymbol{k}_3-\boldsymbol{k}_1)\,v^{(2)}(\boldsymbol{k}_3-\boldsymbol{k}_1,\boldsymbol{k}_1,\boldsymbol{k}_3)}{\omega_{3-1}+\omega_1-\omega_3}-\frac{v^{(1)}(\boldsymbol{k},\boldsymbol{k}_3-\boldsymbol{k}_1,\boldsymbol{k}_2)\,v^{(2)}(\boldsymbol{k}_3-\boldsymbol{k}_1,\boldsymbol{k}_1,\boldsymbol{k}_3)}{\omega_{3-1}+\omega_1-\omega_3}$$

$$-\frac{v^{(1)}(\boldsymbol{k}_2+\boldsymbol{k}_3,\boldsymbol{k}_2,\boldsymbol{k}_3)\,v^{(2)}(\boldsymbol{k},\boldsymbol{k}_1,\boldsymbol{k}+\boldsymbol{k}_1)}{\omega_{2+3}-\omega_2-\omega_3}-\frac{v^{(2)}(\boldsymbol{k},\boldsymbol{k}_2-\boldsymbol{k},\boldsymbol{k}_2)\,v^{(2)}(\boldsymbol{k}_1-\boldsymbol{k}_3,\boldsymbol{k}_3,\boldsymbol{k}_1)}{\omega_{1-3}+\omega_3-\omega_1}$$

$$-\frac{v^{(3)}(-\boldsymbol{k}_2-\boldsymbol{k}_3,\boldsymbol{k}_3,\boldsymbol{k}_2)\,v^{(3)}(\boldsymbol{k},-\boldsymbol{k}-\boldsymbol{k}_1,\boldsymbol{k}_1)}{\omega_{2+3}+\omega_2+\omega_3}-\frac{v^{(3)}(\boldsymbol{k},\boldsymbol{k}_1,-\boldsymbol{k}-\boldsymbol{k}_1)\,v^{(3)}(-\boldsymbol{k}_2-\boldsymbol{k}_3,\boldsymbol{k}_3,\boldsymbol{k}_2)}{\omega_{3+2}+\omega_2+\omega_3},$$

with

$$v^{(1)}(\boldsymbol{k},\boldsymbol{k}_1,\boldsymbol{k}_2) = -2V(-\boldsymbol{k},\boldsymbol{k}_1,\boldsymbol{k}_2)+V(\boldsymbol{k}_1,\boldsymbol{k}_2,\boldsymbol{k}),$$

$$v^{(2)}(\boldsymbol{k},\boldsymbol{k}_1,\boldsymbol{k}_2) = 2(V(\boldsymbol{k},\boldsymbol{k}_1,\boldsymbol{k}_2)-V(-\boldsymbol{k},\boldsymbol{k}_2,\boldsymbol{k}_1)-V(-\boldsymbol{k}_1,\boldsymbol{k}_2,\boldsymbol{k})),$$

$$v^{(3)}(\boldsymbol{k},\boldsymbol{k}_1,\boldsymbol{k}_2) = 2V(\boldsymbol{k},\boldsymbol{k}_1,\boldsymbol{k}_2)+V(\boldsymbol{k}_1,\boldsymbol{k}_2,\boldsymbol{k}),$$

and

$$V(\boldsymbol{k},\boldsymbol{k}_1,\boldsymbol{k}_2) = \lambda(\boldsymbol{k})\,\lambda(\boldsymbol{k}_1)\left[\frac{\rho_2 v_2(\boldsymbol{k},\boldsymbol{k}_1,\boldsymbol{k}_2)}{\rho tn_2(\boldsymbol{k})\,tn_2(\boldsymbol{k}_1)}-\frac{\rho_1 v_1(\boldsymbol{k},\boldsymbol{k}_1,\boldsymbol{k}_2)}{\rho tn_2(\boldsymbol{k})\,tn_2(\boldsymbol{k}_1)}\right],$$

$$v_j(\boldsymbol{k},\boldsymbol{k}_1,\boldsymbol{k}_2) = \frac{1}{8\pi}\left(\frac{\alpha g\omega_2}{2\omega\omega_1}\right)^{\frac{1}{2}}(\boldsymbol{k}\cdot\boldsymbol{k}_1-|\boldsymbol{k}|\,|\boldsymbol{k}_1|tn_j(\boldsymbol{k})\,tn_j(\boldsymbol{k}_1)),$$

$$\omega_j = \omega(\boldsymbol{k}_j),$$

and where

$$\begin{aligned}w^{(2)}(\boldsymbol{k},\boldsymbol{k}_1,\boldsymbol{k}_2,\boldsymbol{k}_3) = {} & W(-\boldsymbol{k},-\boldsymbol{k}_1,\boldsymbol{k}_2,\boldsymbol{k}_3)+W(\boldsymbol{k}_3,\boldsymbol{k}_2,-\boldsymbol{k}_1,-\boldsymbol{k})\\ & -W(-\boldsymbol{k},\boldsymbol{k}_2,-\boldsymbol{k}_1,\boldsymbol{k}_3)-W(-\boldsymbol{k},\boldsymbol{k}_3,\boldsymbol{k}_2,-\boldsymbol{k}_1)\\ & -W(\boldsymbol{k}_2,-\boldsymbol{k}_1,\boldsymbol{k}_3,-\boldsymbol{k})-W(-\boldsymbol{k}_1,\boldsymbol{k}_3,\boldsymbol{k}_2,-\boldsymbol{k}),\end{aligned}$$

with

$$W(\boldsymbol{k},\boldsymbol{k}_1,\boldsymbol{k}_2,\boldsymbol{k}_3) = \lambda(\boldsymbol{k})\,\lambda(\boldsymbol{k}_1)\left(\frac{\rho_2 w_2(\boldsymbol{k},\boldsymbol{k}_1,\boldsymbol{k}_2,\boldsymbol{k}_3)}{\rho tn_2(\boldsymbol{k})\,tn_2(\boldsymbol{k}_1)}+\frac{\rho_1 w_1(\boldsymbol{k},\boldsymbol{k}_1,\boldsymbol{k}_2,\boldsymbol{k}_3)}{\rho tn_1(\boldsymbol{k})\,tn_1(\boldsymbol{k}_1)}\right),$$

and $$w_j(\boldsymbol{k},\boldsymbol{k}_1,\boldsymbol{k}_2,\boldsymbol{k}_3) = \frac{1}{64\pi^2}\left(\frac{\omega_2\,\omega_3}{\omega\omega_1}\right)^{\frac{1}{2}} |\boldsymbol{k}|\,|\boldsymbol{k}_1|[2|\boldsymbol{k}|tn_j(\boldsymbol{k}_1)+2|\boldsymbol{k}_1|tn_j(\boldsymbol{k}) - tn_j(\boldsymbol{k})\,tn_j(\boldsymbol{k}_1)\,(|\boldsymbol{k}+\boldsymbol{k}_2|tn_j(\boldsymbol{k}+\boldsymbol{k}_2)+|\boldsymbol{k}+\boldsymbol{k}_3|tn_j(\boldsymbol{k}+\boldsymbol{k}_3) + |\boldsymbol{k}_1+\boldsymbol{k}_2|tn_j(\boldsymbol{k}_1+\boldsymbol{k}_2)+|\boldsymbol{k}_1+\boldsymbol{k}_3|tn_j(\boldsymbol{k}_1+\boldsymbol{k}_3))],$$

and where

$$y^{(2)}(\boldsymbol{k},\boldsymbol{k}_1,\boldsymbol{k}_2,\boldsymbol{k}_3) = Y(\boldsymbol{k},-\boldsymbol{k}_1,\boldsymbol{k}_2,\boldsymbol{k}_3)+Y(-\boldsymbol{k}_2,\boldsymbol{k}_3,\boldsymbol{k},-\boldsymbol{k}_1)-Y(\boldsymbol{k},\boldsymbol{k}_2,-\boldsymbol{k}_1,\boldsymbol{k}_3) - Y(\boldsymbol{k},\boldsymbol{k}_3,\boldsymbol{k}_2,-\boldsymbol{k}_1)-Y(\boldsymbol{k}_1,\boldsymbol{k}_2,\boldsymbol{k},\boldsymbol{k}_3)-Y(-\boldsymbol{k}_2,-\boldsymbol{k}_1,\boldsymbol{k},\boldsymbol{k}_3),$$

with

$$Y(\boldsymbol{k},\boldsymbol{k}_1,\boldsymbol{k}_2,\boldsymbol{k}_3) = \frac{1}{4}\frac{\lambda(\boldsymbol{k})\,\lambda(\boldsymbol{k}_1)\,\lambda(\boldsymbol{k}_1+\boldsymbol{k}_3)}{tn_1(\boldsymbol{k}_1+\boldsymbol{k}_3)\,tn_2(\boldsymbol{k}_1+\boldsymbol{k}_3)}\left[\frac{y_{11}(\boldsymbol{k},\boldsymbol{k}_1,\boldsymbol{k}_2,\boldsymbol{k}_3)}{tn_1(\boldsymbol{k})\,tn_1(\boldsymbol{k}_1)}+\frac{y_{12}(\boldsymbol{k},\boldsymbol{k}_1,\boldsymbol{k}_2,\boldsymbol{k}_3)}{tn_1(\boldsymbol{k})\,tn_2(\boldsymbol{k}_1)} + \frac{y_{21}(\boldsymbol{k},\boldsymbol{k}_1,\boldsymbol{k}_2,\boldsymbol{k}_3)}{tn_2(\boldsymbol{k})\,tn_1(\boldsymbol{k}_1)}+\frac{y_{22}(\boldsymbol{k},\boldsymbol{k}_1,\boldsymbol{k}_2,\boldsymbol{k}_3)}{tn_2(\boldsymbol{k})\,tn_2(\boldsymbol{k}_1)}\right],$$

$$y_{ij}(\boldsymbol{k},\boldsymbol{k}_1,\boldsymbol{k}_2,\boldsymbol{k}_3) = \frac{1}{4\pi^2}\left(\frac{\omega_2\,\omega_3}{\omega\omega_1}\right)^{\frac{1}{2}}\{|\boldsymbol{k}_1+\boldsymbol{k}_3|\,|\boldsymbol{k}|\,|\boldsymbol{k}_1|tn_i(\boldsymbol{k})\,tn_i(\boldsymbol{k}_1+\boldsymbol{k}_3)\,tn_j(\boldsymbol{k}_1)\,tn_j(\boldsymbol{k}_1+\boldsymbol{k}_3) + (\boldsymbol{k}_1(\boldsymbol{k}_1+\boldsymbol{k}_3))\cdot(\boldsymbol{k}(\boldsymbol{k}_1+\boldsymbol{k}_3))/|\boldsymbol{k}_1+\boldsymbol{k}_3| - (\boldsymbol{k}_1+\boldsymbol{k}_3)\cdot(\boldsymbol{k}_1|\boldsymbol{k}|tn_i(\boldsymbol{k})\,tn_i(\boldsymbol{k}_1+\boldsymbol{k}_3)+\boldsymbol{k}|\boldsymbol{k}_1|tn_j(\boldsymbol{k}_1)\,tn_j(\boldsymbol{k}_1+\boldsymbol{k}_3))\}.$$

Upon the assumption that both depths are approaching infinity, and hence $tn_j(\boldsymbol{k}) \approx 1$, then the Zakharov interaction coefficient can be expressed as

$$T(\boldsymbol{k},\boldsymbol{k}_1,\boldsymbol{k}_2,\boldsymbol{k}_3) = \alpha^2\bar{u}(\boldsymbol{k},\boldsymbol{k}_1,\boldsymbol{k}_2,\boldsymbol{k}_3)+w^{(2)}(\boldsymbol{k},\boldsymbol{k}_1,\boldsymbol{k}_2,\boldsymbol{k}_3)+\tfrac{1}{4}(1-\alpha^2)\,y^{(2)}(\boldsymbol{k},\boldsymbol{k}_1,\boldsymbol{k}_2,\boldsymbol{k}_3),$$

where $$V(\boldsymbol{k},\boldsymbol{k}_1,\boldsymbol{k}_2) = \frac{1}{8\pi}\left(\frac{\alpha g\omega(\boldsymbol{k}_2)}{2\omega(\boldsymbol{k})\,\omega(\boldsymbol{k}_1)}\right)^{\frac{1}{2}}(\boldsymbol{k}\cdot\boldsymbol{k}_1+|\boldsymbol{k}|\,|\boldsymbol{k}_1|),$$

$$W(\boldsymbol{k},\boldsymbol{k}_1,\boldsymbol{k}_2,\boldsymbol{k}_3) = \frac{1}{64\pi^2}\left(\frac{\omega(\boldsymbol{k}_2)\,\omega(\boldsymbol{k}_3)}{\omega(\boldsymbol{k})\,\omega(\boldsymbol{k}_1)}\right)^{\frac{1}{2}}|\boldsymbol{k}|\,|\boldsymbol{k}_1|(2|\boldsymbol{k}|+2|\boldsymbol{k}_1|-|\boldsymbol{k}_1+\boldsymbol{k}_2| - |\boldsymbol{k}_1+\boldsymbol{k}_3|-|\boldsymbol{k}+\boldsymbol{k}_2|-|\boldsymbol{k}+\boldsymbol{k}_3|),$$

and $$Y(\boldsymbol{k},\boldsymbol{k}_1,\boldsymbol{k}_2,\boldsymbol{k}_3) = \frac{1}{4\pi^2}\left(\frac{\omega(\boldsymbol{k}_2)\,\omega(\boldsymbol{k}_3)}{\omega(\boldsymbol{k})\,\omega(\boldsymbol{k}_1)}\right)^{\frac{1}{2}}(|\boldsymbol{k}_1+\boldsymbol{k}_3|\,|\boldsymbol{k}|\,|\boldsymbol{k}_1|+\boldsymbol{k}_1\cdot(\boldsymbol{k}_1+\boldsymbol{k}_3) \times\boldsymbol{k}\cdot(\boldsymbol{k}_1+\boldsymbol{k}_3)/|\boldsymbol{k}_1+\boldsymbol{k}_3|-(\boldsymbol{k}_1+\boldsymbol{k}_3)\cdot(\boldsymbol{k}_1|\boldsymbol{k}|+\boldsymbol{k}|\boldsymbol{k}_1|)),$$

with $v^{(j)}(\boldsymbol{k},\boldsymbol{k}_1,\boldsymbol{k}_2,\boldsymbol{k}_3)$ being defined as above in terms of the infinite depth $V(\boldsymbol{k},\boldsymbol{k}_1,\boldsymbol{k}_2,\boldsymbol{k}_3)$ and $\bar{u}(\boldsymbol{k},\boldsymbol{k}_1,\boldsymbol{k}_2,\boldsymbol{k}_3)$ having the same definition as $u(\boldsymbol{k},\boldsymbol{k}_1,\boldsymbol{k}_2,\boldsymbol{k}_3)$ in terms of the infinite-depth definition of $v^{(j)}$. Similarly $y^{(2)}$ and $w^{(2)}$ are defined as above in terms of the infinite-depth definitions of $W(\boldsymbol{k},\boldsymbol{k}_1,\boldsymbol{k}_2,\boldsymbol{k}_3)$ and $Y(\boldsymbol{k},\boldsymbol{k}_1,\boldsymbol{k}_2,\boldsymbol{k}_3)$.

A.2. *Symmetries in the depths in the Boussinesq limit*

It can be shown that, in the Boussinesq limit, if the values of the two depths are interchanged the Zakharov interaction coefficient is unchanged and hence the resultant growth rates remain the same.

As $\rho_1 = \rho_2$ then by inspection $\lambda(\boldsymbol{k})$ and $\omega(\boldsymbol{k})$ are symmetric in d_j. That is if d_1 and d_2 are interchanged these quantities are unaltered. It therefore follows that $W(\boldsymbol{k},\boldsymbol{k}_1,\boldsymbol{k}_2,\boldsymbol{k}_3)$ and $Y(\boldsymbol{k},\boldsymbol{k}_1,\boldsymbol{k}_2,\boldsymbol{k}_3)$ are symmetric as well, and hence $y^{(2)}(\boldsymbol{k},\boldsymbol{k}_1,\boldsymbol{k}_2,\boldsymbol{k}_3)$ and $w^{(2)}(\boldsymbol{k},\boldsymbol{k}_1,\boldsymbol{k}_2,\boldsymbol{k}_3)$ are. Alternatively, if d_1 and d_2 are interchanged then $V(\boldsymbol{k},\boldsymbol{k}_1,\boldsymbol{k}_2)$ experiences a change in sign. This change of sign is propagated through to the $v^{(j)}(\boldsymbol{k},$

$\boldsymbol{k}_1, \boldsymbol{k}_2$) terms but as the Zakharov coefficient is dependent upon only the product of two of these terms then it is unchanged, hence the Zakharov interaction coefficient is invariant under the interchanging of the depths in the Boussinesq limit.

Appendix B. Coefficient of the cubic term for the nonlinear Schrödinger equation

Under the assumption that $tn_j(\boldsymbol{p}) \approx |\boldsymbol{p}|d_j$ and that $\omega(\boldsymbol{k}_0+\boldsymbol{p})$ can be approximated by $\omega(\boldsymbol{k}_0)+\boldsymbol{p}\cdot\boldsymbol{c}_g$, then

$$T(\boldsymbol{k}_0+\boldsymbol{p}, \boldsymbol{k}_0+\boldsymbol{p}_1, \boldsymbol{k}_0+\boldsymbol{p}_2, \boldsymbol{k}_0+\boldsymbol{p}_3) \approx \mu_0(\boldsymbol{k}_0)+\mu_1(\boldsymbol{k}_0, \boldsymbol{p}_3-\boldsymbol{p}_1),$$

where

$$\mu_0(\boldsymbol{k}_0) = \frac{k_0^3\lambda^2(\boldsymbol{k}_0)}{16\pi^2\rho}\left\{\frac{(\rho_2(1-3/tn_2^2(\boldsymbol{k}_0))-\rho_1(1-3/tn_1^2(\boldsymbol{k}_0)))^2}{2(\rho_2 tn_2(\boldsymbol{k}_0)+\rho_1 tn_1(\boldsymbol{k}_0))}\right.$$
$$\left.+\frac{2\rho_2(2-1/tn_2^2(\boldsymbol{k}_0))}{tn_2(\boldsymbol{k}_0)}+\frac{2\rho_1(2-1/tn_1^2(\boldsymbol{k}_0))}{tn_1(\boldsymbol{k}_0)}\right\}+\frac{k_0^3\,\omega^2(\boldsymbol{k}_0)\,(\chi_1+\chi_2)}{k_0\,c_g^2-\omega_p^2}+k_0^3\,\chi_3,$$

$$\mu_1(\boldsymbol{k}_0, \boldsymbol{p}) = \frac{q^2\boldsymbol{k}_0^3\,\omega^2(\boldsymbol{k}_0)\,(\chi_1\,\omega_p^2+\chi_2\,k_0^2\,c_g^2)}{(k_0^2\,c_g^2-\omega_p^2)\,(k_0^2\,c_g^2\,p^2-\omega_p^2|\boldsymbol{p}|^2)},$$

and where

$$\chi_1 = \frac{\lambda(\boldsymbol{k}_0)}{4\pi^2(\rho_2/k_0\,d_2+\rho_1/k_0\,d_1)}\left\{\frac{1}{\rho_1/k_0\,d_1+\rho_2/k_0\,d_2}\left(\frac{\rho_2}{k_0\,d_2\,tn_2(\boldsymbol{k}_0)}-\frac{\rho_1}{k_0\,d_1\,tn_1(\boldsymbol{k}_0)}\right)^2\right.$$
$$\left.-\frac{c_g\,\lambda\,(\boldsymbol{k}_0)\,k_0}{\omega(\boldsymbol{k}_0)\,\rho}\left(\frac{\rho_2}{tn_2(\boldsymbol{k}_0)\,k_0\,d_2}-\frac{\rho_1}{tn_1(\boldsymbol{k}_0)\,k_0\,d_1}\right)\left[\rho_2\left(1-\frac{1}{tn_2^2(\boldsymbol{k}_0)}\right)-\rho_1\left(1-\frac{1}{tn_1^2(\boldsymbol{k}_0)}\right)\right]\right\}$$

$$\chi_2 = \frac{\lambda^2(\boldsymbol{k}_0)}{16\pi^2(\rho_2/k_0\,d_2+\rho_1/k_0\,d_1)}\left[\rho_2\left(1-\frac{1}{tn_2^2(\boldsymbol{k}_0)}\right)-\rho_1\left(1-\frac{1}{tn_1^2(\boldsymbol{k}_0)}\right)\right]^2,$$

$$\chi_3 = -\frac{\rho_1\rho_2\,\lambda^2(\boldsymbol{k}_0)}{4\pi^2\rho}\left(\frac{(1/tn_1(\boldsymbol{k}_0)+1/tn_2(\boldsymbol{k}_0))^2}{\rho_2\,k_0\,d_1+\rho_1\,k_0\,d_2}\right), \quad \text{and} \quad \omega_p^2 = \frac{(\rho_2-\rho_1)\,gk_0}{\rho_1/k_0\,d_1+\rho_2/k_0\,d_2}.$$

The first term of $\mu_0(\boldsymbol{k}_0)$ gives the usual Stokes correction to the phase velocity, once multiplied by B_0^2, while the remaining terms represent the wave-induced 'drift velocity' and reduce to the expression given by Davey & Stewartson (1974) for the surface wave case.

For the infinite depths these reduce to

$$\mu_0(\boldsymbol{k}_0) = \frac{k_0^3}{8\pi^2}(1+\alpha^2) \quad \text{with} \quad \mu_1(\boldsymbol{k}_0, \boldsymbol{p}) = 0.$$

Appendix C

C.1. *Large wavenumber Kelvin–Helmholtz instability*

As was shown in §6 the Zakharov equation was inadequate in describing the Kelvin–Helmholtz instability induced by a periodic wave. In this section we shall show that this limitation is due to the exclusion of the non-resonant terms (the terms which rapidly vary with time) of (2.20), as it was assumed that the resonant term would always be dominant. This term, which gives the Zakharov equation, is dominant only for perturbation wavenumbers near the region of resonance, that is near the 'figure of 8'. Elsewhere these other terms are of equal importance.

For simplicity we shall confine the discussion to the case of infinite depths and to the Boussinesq limit. Here the second-order terms vanish and (2.20) can be obtained from (2.18) with no restriction on the timescale for B, i.e. set

$$b(\boldsymbol{k},t) = \epsilon B(\boldsymbol{k},t)\,\mathrm{e}^{-\mathrm{i}\omega(\boldsymbol{k})t}.$$

The terms $T_j(\boldsymbol{k},\boldsymbol{k}_1,\boldsymbol{k}_2,\boldsymbol{k}_3)$ are defined below for this particular case.

First, let us investigate the contribution of the non-resonant terms to the basic periodic wave solution. Assuming the form

$$B(\boldsymbol{k},t) = A_1(t)\,\delta(\boldsymbol{k}-\boldsymbol{k}_0)+A_2(t)\,\delta(\boldsymbol{k}+\boldsymbol{k}_0)+A_3\,\delta(\boldsymbol{k}-3\boldsymbol{k}_0)+A_4\,\delta(\boldsymbol{k}+3\boldsymbol{k}_0) \tag{C 1}$$

and by substitution into (2.20) it is possible to solve for A_j under the assumption $A_j \ll A_1$, $i \neq 1$, and hence the nonlinear terms are in A_1 alone to leading order. Reverting to physical space gives

$$\begin{aligned} k_0\,\eta(\boldsymbol{x},t) &= k_0\,a\left(1-(k_0\,a)^2\frac{\pi^2}{2k_0^3}T_3(-\boldsymbol{k}_0,\boldsymbol{k}_0,\boldsymbol{k}_0,\boldsymbol{k}_0)\right)\cos\theta \\ &-2(k_0\,a)^3\,\pi^2\omega(\boldsymbol{k}_0)\left(\frac{3\omega(\boldsymbol{k}_0)}{\omega(3\boldsymbol{k}_0)}\right)\left(\frac{T_1(3\boldsymbol{k}_0,\boldsymbol{k}_0,\boldsymbol{k}_0,\boldsymbol{k}_0)}{\omega(3\boldsymbol{k}_0)-3\omega(\boldsymbol{k}_0)}+\frac{T_4(-3\boldsymbol{k}_0,\boldsymbol{k}_0,\boldsymbol{k}_0,\boldsymbol{k}_0)}{\omega(3\boldsymbol{k}_0)+3\omega(\boldsymbol{k}_0)}\right)\cos 3\theta, \end{aligned} \tag{C 2}$$

where $\theta = \boldsymbol{k}_0\cdot\boldsymbol{x}-\omega(\boldsymbol{k}_0)\,(1+2(k_0\,a)^2\,\pi^2 T_2(\boldsymbol{k}_0,\boldsymbol{k}_0,\boldsymbol{k}_0,\boldsymbol{k}_0)/k_0^3)\,t = \boldsymbol{k}_0\cdot\boldsymbol{x}-\bar{\omega}_0\,t.$

As can be seen the interaction coefficient from the resonant term T_2 appears only in the nonlinear correction to the phase velocity. The non-resonant terms modify the shape of the wave, either by changing the amplitude of the fundamental or by generating a harmonic.

To investigate how the non-resonant terms effect the stability of this basic wave set

$$B(\boldsymbol{k},t) = B_s(\boldsymbol{k},t)+\hat{B}(\boldsymbol{k},t), \tag{C 3}$$

where B_s is defined as in (4.1) and (4.2). Upon substitution into (2.20), and linearizing in $\hat{B}$, one obtains

$$\begin{aligned} \mathrm{i}\hat{B}_t(\boldsymbol{k}) = {} & (T_1(\boldsymbol{k},\boldsymbol{k}_0,\boldsymbol{k}_0,\boldsymbol{k}-2\boldsymbol{k}_0)+T_1(\boldsymbol{k},\boldsymbol{k}_0,\boldsymbol{k}-2\boldsymbol{k}_0,\boldsymbol{k}_0)+T_1(\boldsymbol{k},\boldsymbol{k}-2\boldsymbol{k}_0,\boldsymbol{k}_0,\boldsymbol{k}_0)) \\ & \times B_0^2\hat{B}(\boldsymbol{k}-2\boldsymbol{k}_0)\,\mathrm{e}^{\mathrm{i}(\omega(\boldsymbol{k})-\omega(\boldsymbol{k}-2\boldsymbol{k}_0)-2\bar{\omega}_0))t} \\ & +(T_2(\boldsymbol{k},\boldsymbol{k}_0,\boldsymbol{k}_0,\boldsymbol{k})+T_2(\boldsymbol{k},\boldsymbol{k}_0,\boldsymbol{k},\boldsymbol{k}_0))\,B_0^2\hat{B}(\boldsymbol{k}) \\ & +T_2(\boldsymbol{k},2\boldsymbol{k}_0-\boldsymbol{k},\boldsymbol{k}_0,\boldsymbol{k}_0)\,B_0^2\hat{B}^*(2\boldsymbol{k}_0-\boldsymbol{k})\,\mathrm{e}^{\mathrm{i}(\omega(\boldsymbol{k})+\omega(\boldsymbol{k}-2\boldsymbol{k}_0)-2\bar{\omega}_0)t} \\ & +(T_3(\boldsymbol{k},\boldsymbol{k}_0,-\boldsymbol{k},\boldsymbol{k}_0)+T_3(\boldsymbol{k},-\boldsymbol{k},\boldsymbol{k}_0,\boldsymbol{k}_0))\,B_0^2\hat{B}^*(-\boldsymbol{k})\,\mathrm{e}^{2\mathrm{i}(\omega(\boldsymbol{k}))t} \\ & +T_3(\boldsymbol{k},\boldsymbol{k}_0,\boldsymbol{k}_0,\boldsymbol{k}+2\boldsymbol{k}_0)\,B_0^2\hat{B}(\boldsymbol{k}+2\boldsymbol{k}_0)\,\mathrm{e}^{\mathrm{i}(\omega(\boldsymbol{k})-\omega(\boldsymbol{k}+2\boldsymbol{k}_0)+2\bar{\omega}_0)t} \\ & +(T_4(\boldsymbol{k},\boldsymbol{k}_0,\boldsymbol{k}_0,-2\boldsymbol{k}_0-\boldsymbol{k})+T_4(\boldsymbol{k},\boldsymbol{k}_0,-\boldsymbol{k}-2\boldsymbol{k}_0,\boldsymbol{k}_0) \\ & +T_4(\boldsymbol{k},-\boldsymbol{k}-2\boldsymbol{k}_0,\boldsymbol{k}_0,\boldsymbol{k}_0)) \\ & \times B_0^2\hat{B}(-\boldsymbol{k}-2\boldsymbol{k}_0)\,\mathrm{e}^{\mathrm{i}(\omega(\boldsymbol{k})+\omega(\boldsymbol{k}+2\boldsymbol{k}_0)+2\bar{\omega}_0)t}. \end{aligned} \tag{C 4}$$

Upon expanding the interaction coefficients to leading order for large $|\boldsymbol{k}|/k_0$, one obtains

$$\begin{aligned} \hat{B}_t(\boldsymbol{k}) = {} & \mathrm{i}\frac{B_0^2\,k_0^{\frac{3}{2}}\,k^2}{16\pi^2|\boldsymbol{k}|^{\frac{1}{2}}}\{(\hat{B}(\boldsymbol{k}-2\boldsymbol{k}_0)\,\mathrm{e}^{-2\mathrm{i}\bar{\omega}_0 t}+2\hat{B}(\boldsymbol{k})+\hat{B}(\boldsymbol{k}+2\boldsymbol{k}_0)\,\mathrm{e}^{2\mathrm{i}\bar{\omega}_0 t}) \\ & +\mathrm{e}^{2\mathrm{i}\omega(\boldsymbol{k})t}(\hat{B}^*(-\boldsymbol{k}+2\boldsymbol{k}_0)\,\mathrm{e}^{-2\mathrm{i}\bar{\omega}_0 t}+2\hat{B}^*(-\boldsymbol{k})+\hat{B}^*(-\boldsymbol{k}-2\boldsymbol{k}_0)\,\mathrm{e}^{2\mathrm{i}\bar{\omega}_0 t})\}, \end{aligned} \tag{C 5}$$

where the approximation that

$$|\omega(\boldsymbol{k} \pm 2\boldsymbol{k}_0) - \omega(\boldsymbol{k})|\, t \ll 1$$

is made, implying that $\omega(\boldsymbol{k}_0)\, t \ll |\boldsymbol{k}|/k_0$. This restriction is not severe as we shall see that once the period of time has elapsed such that this is no longer valid, neither is the assumption that $\hat{B}$ is small, owing to the exponential growth from the instability. Note that all the terms of (C 4) are of a similar size in this limit of large $|\boldsymbol{k}|/k_0$.

Taking the inverse Fourier transform gives

$$\int_{-\infty}^{\infty} \left(\mathrm{i}(\hat{B}_t(\boldsymbol{k}) + \frac{B_0^2 k_0^2}{4\pi^2} \cos^2\theta \frac{k^2}{|\boldsymbol{k}|^{\frac{1}{2}}} (\hat{B}(\boldsymbol{k}) + \mathrm{e}^{2\mathrm{i}\omega(\boldsymbol{k})t} \hat{B}^*(-\boldsymbol{k})) \right) \mathrm{e}^{\mathrm{i}\boldsymbol{k}\cdot\boldsymbol{x}}\, \mathrm{d}\boldsymbol{k} = 0,$$

and assuming the perturbation comprises of a pair of waves of wavenumber $\pm \boldsymbol{p}$

$$\hat{B}(\boldsymbol{k}, t) = B_+(t)\, \delta(\boldsymbol{k} - \boldsymbol{p}) + B_-(t)\, \delta(\boldsymbol{k} + \boldsymbol{p}), \tag{C 6}$$

the set of equations

$$\mathrm{i}B_{\pm, t} = -\frac{B_0^2 k_0^{\frac{3}{2}} p^2}{4\pi^2 |\boldsymbol{p}|^{\frac{1}{2}}} \cos^2\theta (B_\pm + \mathrm{e}^{2\mathrm{i}\omega(\boldsymbol{p})t} B_\mp^*) \tag{C 7}$$

is obtained by keeping θ fixed, which is valid for $|\boldsymbol{p}|/k_0$ large enough. This describes the local behaviour of $B_\pm$ at a given phase angle of the main wave. Solving as before one obtains (6.2) to leading order where $\omega(\boldsymbol{k}_0)$ is replaced by $\bar{\omega}_0$, i.e. taking into account the nonlinear correction to the phase velocity.

If only the resonant term is used, i.e. the Zakharov equation, one obtains

$$\frac{\sigma}{\omega(\boldsymbol{k}_0)} = \left(\frac{3p^4}{64|\boldsymbol{p}|k_0^3} (k_0 a)^4 + \frac{|\boldsymbol{p}|}{k_0} - \frac{p^2}{2k_0^2} (k_0 a)^2 \right)^{\frac{1}{2}}, \tag{C 8}$$

for a band of instability such that

$$\frac{8}{3} < \frac{p^2}{k_0 |\boldsymbol{p}|} (k_0 a)^2 < 8,$$

in agreement with earlier results.

With the inclusion of the off-resonance terms we have successfully rederived the growth rates for wave-induced Kelvin–Helmholtz instability.

C.2. *Interaction coefficients T_j*

For the case of the Boussinesq limit, and when both depths are infinite, the interaction coefficients are defined as:

$$\begin{aligned}
T_1(\boldsymbol{k}, \boldsymbol{k}_1, \boldsymbol{k}_2, \boldsymbol{k}_3) = & -W(-\boldsymbol{k}, \boldsymbol{k}_1, \boldsymbol{k}_2, \boldsymbol{k}_3) + W(\boldsymbol{k}_1, \boldsymbol{k}_2, -\boldsymbol{k}, \boldsymbol{k}_3) - \tfrac{1}{4}[Y(\boldsymbol{k}, \boldsymbol{k}_1, \boldsymbol{k}_2, \boldsymbol{k}_3) \\
& - Y(-\boldsymbol{k}_2, \boldsymbol{k}_1, \boldsymbol{k}, \boldsymbol{k}_3)],
\end{aligned}$$

$$\begin{aligned}
T_2(\boldsymbol{k}, \boldsymbol{k}_1, \boldsymbol{k}_2, \boldsymbol{k}_3) = & -W(-\boldsymbol{k}, \boldsymbol{k}_3, \boldsymbol{k}_2, -\boldsymbol{k}_1) - W(-\boldsymbol{k}, \boldsymbol{k}_2, -\boldsymbol{k}_1, \boldsymbol{k}_3) + W(-\boldsymbol{k}, -\boldsymbol{k}_1, \boldsymbol{k}_2, \boldsymbol{k}_3) \\
& + W(\boldsymbol{k}_2, \boldsymbol{k}_3, -\boldsymbol{k}, -\boldsymbol{k}_1) - W(\boldsymbol{k}_2, -\boldsymbol{k}_1, -\boldsymbol{k}, \boldsymbol{k}_3) - W(\boldsymbol{k}_3, -\boldsymbol{k}_1, \boldsymbol{k}_2, -\boldsymbol{k}) \\
& + \tfrac{1}{4}[-Y(\boldsymbol{k}, \boldsymbol{k}_3, \boldsymbol{k}_2, -\boldsymbol{k}_1) - Y(\boldsymbol{k}, \boldsymbol{k}_2, -\boldsymbol{k}_1, \boldsymbol{k}_3) + Y(\boldsymbol{k}, -\boldsymbol{k}_1, \boldsymbol{k}_2, \boldsymbol{k}_3) \\
& - Y(\boldsymbol{k}_1, \boldsymbol{k}_2, \boldsymbol{k}, \boldsymbol{k}_3) + Y(-\boldsymbol{k}_2, \boldsymbol{k}_3, \boldsymbol{k}, -\boldsymbol{k}_1) - Y(-\boldsymbol{k}_2, -\boldsymbol{k}_1, \boldsymbol{k}, \boldsymbol{k}_3)],
\end{aligned}$$

$$\begin{aligned}
T_3(\boldsymbol{k}, \boldsymbol{k}_1, \boldsymbol{k}_2, \boldsymbol{k}_3) = & -W(-\boldsymbol{k}, \boldsymbol{k}_3, -\boldsymbol{k}_2, -\boldsymbol{k}_1) + 2W(-\boldsymbol{k}, -\boldsymbol{k}_1, \boldsymbol{k}_3, -\boldsymbol{k}_2) \\
& + W(-\boldsymbol{k}_1, -\boldsymbol{k}_2, \boldsymbol{k}_3, -\boldsymbol{k}) - 2W(-\boldsymbol{k}_1, \boldsymbol{k}_3, -\boldsymbol{k}, -\boldsymbol{k}_2) \\
& + \tfrac{1}{4}[-Y(\boldsymbol{k}, \boldsymbol{k}_3, -\boldsymbol{k}_2, -\boldsymbol{k}_1) + Y(\boldsymbol{k}, -\boldsymbol{k}_1, \boldsymbol{k}_3, -\boldsymbol{k}_2) + Y(\boldsymbol{k}, -\boldsymbol{k}_1, -\boldsymbol{k}_2, \boldsymbol{k}_3) \\
& - Y(\boldsymbol{k}_2, \boldsymbol{k}_3, \boldsymbol{k}, -\boldsymbol{k}_1) + Y(\boldsymbol{k}_2, -\boldsymbol{k}_1, \boldsymbol{k}, \boldsymbol{k}_3) - Y(-\boldsymbol{k}_3, -\boldsymbol{k}_1, \boldsymbol{k}, -\boldsymbol{k}_2)],
\end{aligned}$$

$$\begin{aligned}
T_4(\boldsymbol{k}, \boldsymbol{k}_1, \boldsymbol{k}_2, \boldsymbol{k}_3) = & \; W(\boldsymbol{k}, \boldsymbol{k}_1, \boldsymbol{k}_2, \boldsymbol{k}_3) + W(\boldsymbol{k}_1, \boldsymbol{k}_2, \boldsymbol{k}_3, \boldsymbol{k}) \\
& + \tfrac{1}{4}[Y(\boldsymbol{k}_2, -\boldsymbol{k}_1, \boldsymbol{k}, -\boldsymbol{k}_3) + Y(\boldsymbol{k}, -\boldsymbol{k}_1, -\boldsymbol{k}_2, -\boldsymbol{k}_3)].
\end{aligned}$$

REFERENCES

CRAIK, A. D. D. 1968 Resonant gravity-wave interactions in a shear flow. *J. Fluid Mech.* **34**, 531–549.

CRAIK, A. D. D. 1985 *Wave Interactions and Fluid Flows*. Cambridge University Press.

CRAWFORD, D. R., LAKE, B. M., SAFFMAN, P. G. & YUEN, H. C. 1981 Stability of weakly nonlinear deep-water waves in two and three dimensions. *J. Fluid Mech.* **105**, 177–191.

DAVEY, A. & STEWARTSON, K. 1974 On three-dimensional packets of surface waves. *Proc. R. Soc. Lond.* A **338**, 101–110.

DRAZIN, P. G. & REID, W. H. 1981 *Hydrodynamic Stability*. Cambridge University Press.

GRIMSHAW, R. H. J. & PULLIN, D. I. 1985 Stability of finite-amplitude interfacial waves. Part 1. Modulational instability for small-amplitude waves. *J. Fluid Mech.* **160**, 297–315.

HOLYER, J. H. 1979 Large amplitude progressive interfacial waves. *J. Fluid Mech.* **93**, 433–448.

LONGUET-HIGGINS, M. S. 1978*a* The instability of gravity waves of finite amplitude in deep water. I. Superharmonics. *Proc. R. Soc. Lond.* A **360**, 471–488.

LONGUET-HIGGINS, M. S. 1978*b* The instability of gravity waves of finite amplitude in deep water. II. Subharmonics. *Proc. R. Soc. Lond.* A **360**, 489–505.

MCLEAN, J. W. 1982*a* Instabilities of finite-amplitude water waves. *J. Fluid Mech.* **114**, 315–330.

MCLEAN, J. W. 1982*b* Instabilities of finite-amplitude gravity water waves on water of finite depth. *J. Fluid Mech.* **114**, 331–341.

PHILLIPS, O. M. 1960 On the dynamics of unsteady waves of finite amplitude. Part 1. The elementary interactions. *J. Fluid Mech.* **9**, 193–217.

PHILLIPS, O. M. 1981 Wave interactions – the evolution of an idea. *J. Fluid Mech.* **106**, 215–227.

PULLIN, D. I. & GRIMSHAW, R. H. J. 1983*a* Nonlinear interfacial progressive waves near a boundary in a Boussinesq fluid. *Phys. Fluids* **26**, 897–905.

PULLIN, D. I. & GRIMSHAW, R. H. J. 1983*b* Interfacial progressive waves in a two layer shear flow. *Phys. Fluids* **26**, 1731–1739.

PULLIN, D. I. & GRIMSHAW, R. H. J. 1985 Stability of finite-amplitude interfacial waves. Part 2. Numerical results. *J. Fluid Mech.* **160**, 317–386.

PULLIN, D. I. & GRIMSHAW, R. H. J. 1986 Stability of finite-amplitude interfacial waves. Part 3. The effect of basic current shear for one-dimensional instabilities. *J. Fluid Mech.* **172**, 277–306.

SAFFMAN, P. G. & YUEN, H. C. 1982 Finite amplitude interfacial waves in the presence of a current. *J. Fluid Mech.* **123**, 459–476.

STIASSNIE, M. & SHEMER, L. 1984 On modifications of the Zakharov equation for surface gravity waves. *J. Fluid Mech.* **143**, 47–67.

WHITHAM, G. B. 1967 Nonlinear dispersion of water waves. *J. Fluid Mech.* **27**, 399–412.

YUEN, H. C. 1984 Nonlinear dynamics of interfacial waves. *Physica* **12D**, 71–82.

YUEN, H. C. & LAKE, B. M. 1982 Nonlinear dynamics of deep-water gravity waves. *Adv. Appl. Mech.* **22**, 67–229.

ZAKHAROV, V. E. 1968 Stability of periodic waves of finite amplitude on the surface of a deep fluid. *Zh. Prikl. Mekh. Fiz.* **9**, 86. (Engl. transl. *J. Appl. Mech. Tech. Phys.* **2**, 190–194.)

ZAKHAROV, V. E. & KHARITONOV, V. G. 1970 Instability of monochromatic waves on the surface of a liquid of arbitrary depth. *Zh. Prikl. Mekh. Fiz.* **5**, 45–49 (Engl. transl. *J. Appl. Mech. Tech. Phys.* **11**, 747–751).